

8 DMT modulation for VLC

Klaus-Dieter Langer

8.1

Introduction

Optical free space communication using visible radiation, i.e. light, has been known for a very long time. Some early examples are signaling using fire, the *Heliograph* using sunlight, which is directed to the receiver by means of a mirror, or the *Photophone* invented by Graham Bell (1880). Due to the outstanding success of radio technologies and due to their intrinsic benefits, up to now optical free space communication has remained a niche technology. One of such niche applications took advantage of the immunity from interception, namely the so-called directed transmission for military aims during World War 2 and later on. Different approaches such as optical wireless communication (OWC) using fluorescent tubes are also well recorded in the patent literature but have never achieved a breakthrough.

A revival of this way of wireless communication has come about with the advent of visible light LEDs of increasingly high optical power. While their application initially was limited to signaling (e.g. telltale or warning light), at the turn of the millennium it became apparent that in future lighting would be dominated by LEDs. Henceforth, there has been growing interest in applications using LED-based OWC, or which combine the functions of lighting and optical wireless data transmission. At the same time, the common term *Visible Light Communications* (VLC) was coined for this kind of communication. The major reasons for the steadily rising interest in VLC are the lifetime and improved optical power of white light LEDs particularly, and their progressive adoption, as well as the simplicity of LED modulation via their driving current at a modulation bandwidth in the lower MHz range, see e.g. [1–3]. Moreover, the proliferation of mobile applications using radio frequencies has accentuated concerns about the adequate availability of radio-frequency bands and the limits of transmission capacity in current wireless networks, as well as the related data security issues. In this respect, VLC can offer an additional option for local wireless data links where radio links are not desired or not possible [4–6].

The building blocks of a generic VLC system are shown in Fig. 8.1. Regarding the historical background of VLC and its use for transferring messages via schemes such as the Morse code, it seems to be obvious and straightforward to apply plain on-off keying (OOK). Indeed, simple experimental VLC systems use OOK realized by intensity modulation (IM). At the receiving side, direct detection is applied using a photodetector for optoelectronic signal conversion. While image sensors can be used in

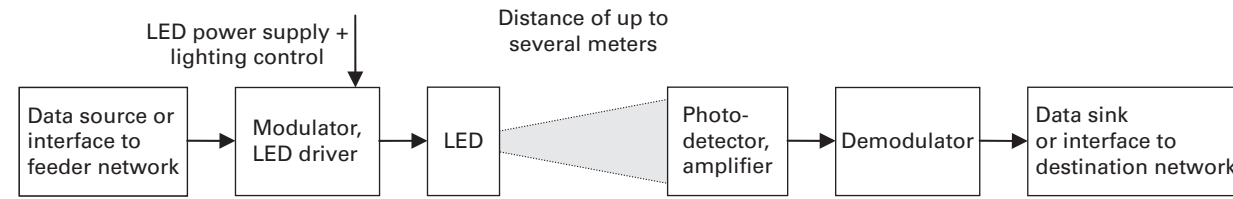


Figure 8.1 Building blocks of a basic short-haul visible light transmission system.

low-speed systems (cf. [3]), high data rates call for a Si-PIN or avalanche photodiode (APD) as the device for optical detection. In such configurations based on OOK and white light LEDs intended for lighting, transmission speeds of e.g. 230 Mbit/s have been achieved [7].

This chapter is focused on indoor applications of VLC, where LEDs are used as an optical source for either (pure) high-speed data transmission or for lighting plus data transmission at bit rates in the upper Mbit/s range (up to Gbit/s speed). Sample applications of high-capacity indoor links are presented in the next section. Given the modulation bandwidth offered by current LEDs, in contrast to the OOK case the targeted data rates require advanced and highly spectrum efficient solutions for modulation, such as discrete multitone (DMT), which is addressed in this chapter. In fact, the highest bit rates demonstrated so far in a single VLC channel use such modulation schemes [8–11].

When considering VLC systems as mentioned before, the reach should be within the range of several meters (say up to ~20 m). Depending on applications such as data broadcast, video streaming or file transfer, either unidirectional or bidirectional links are required in point-to-point (P-t-P) or point-to-multipoint (P-t-MP) configuration. Additional requirements in the dual-use case of LEDs for lighting and data transmission include illumination according to the well-established lighting standards and features without restrictions, no flickering light, dimming, etc., cf. [12]. However, it has to be mentioned that, for instance, the present version of the IEEE standard on VLC only considers OOK, variable pulse position modulation (VPPM), and color shift keying (CSK) as a special scheme with respect to multiple optical sources of different color, while DMT is not yet included [13–15].

The chapter is structured in the following way. We continue with a brief discussion of some typical indoor application scenarios, as they are of interest for the general public and in industrial sectors. The next section is devoted to the relevant characteristics of white light LEDs as the key VLC element. In addition, the optical wireless channel capacity is addressed, as well as LED modulation for exploiting the capacity, and major issues such as the effect of LED non-linearity.

The main part of this chapter presents the DMT modulation scheme and variants thereof, including related signal processing as well as bit and power loading. Substantial effects and consequences such as signal clipping, peak-to-average power ratio (PAPR) and the influence of channel variation are detailed in this section. Subsequently, several recently proposed improvements of the DMT modulation scheme are introduced and various approaches are compared. On that basis, Section 8.6 examines important aspects of system design, implementation issues, and demonstrations in step with actual practice. A summary and an outlook are included at the end of this chapter.

8.2

Indoor application scenarios

VLC can be applied in quite different scenarios. In particular, when high data rates are considered the type of link between transmitter (Tx) and receiver (Rx) is crucial.

According to the mode of propagation of light, there are two generic types of indoor optical wireless links. Firstly the *directed link*, which relies on a non-blocked line-of-sight (LOS) between a highly directed Tx and a narrow field-of-view (FOV) Rx. Secondly, the *diffuse link*, characterized by a wide-beam Tx and a large FOV Rx, where the non-LOS light path relies on numerous signal reflections off the walls and surfaces of objects present in the room [16].

LOS links experience minimal path loss, are rather free from multipath induced signal distortion, and are able to diminish the influence of ambient light. As long as the LOS is not blocked, the link performance only depends on the available power budget. Hence, very high transmission rates are shown to be possible. On the other hand, LOS links require alignment of transceivers and generically provide a very small coverage.

A diffuse link operates entirely without LOS, which results in an increased robustness against shadowing and support of high user mobility within a large coverage area. Thus, a diffuse link scenario enables P-t-MP communication and in general is most desirable from the user's point of view. This is why it evoked much interest from the research community. However, diffuse links suffer from high optical path loss (i.e., they require larger optical powers) and are seriously limited by inter-symbol interference (ISI) because of multipath dispersion, which presents a major degradation factor at higher transmission rates. Beside the power budget, the achievable transmission rate depends also on room characteristics such as size, reflection coefficients of surfaces, etc. It should be mentioned that the effects of multipath fading are negligible in OWC due to square-law detection on a photodiode (PD) of huge size compared to the incoming signal wavelength. This greatly simplifies the link design.

Many VLC applications call for combining the mobility of a diffuse link and the high-speed capability of a LOS link. In order to benefit from the advantages of both connection types, a non-directed LOS (NLOS) link is frequently considered as an alternative. In such a link, LOS and diffuse signal components are simultaneously present at the Rx (assuming a non-blocked LOS path). The equivalent channel response as shown in Fig. 8.2 is characterized by high dynamics in both bandwidth and gain, depending above all, on the LOS prominence. Consequently, the ratio of LOS and diffuse signal components at the Rx, often described by the Rician K -factor, strongly influences achievable data rate,

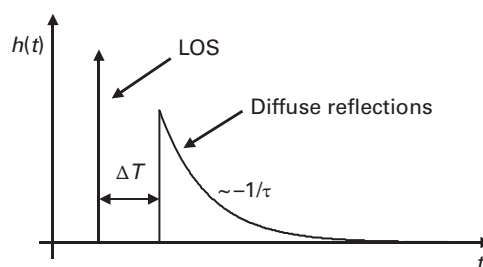


Figure 8.2 Channel impulse response $h(t)$ as a superposition of the LOS and diffuse channel responses, where ΔT indicates the delay between arrival of the LOS signal and the first reflection at the receiver; $1/\tau$ is the decay constant of the diffuse channel.

Table 8.1 Comparison of commonly present link configurations for optical wireless indoor systems.

Link type	Directed LOS	Non-directed LOS	Diffuse
Link rate	highest	high	moderate
Beam pointing	yes	coarse	no
Beam blocking	yes	relaxed	no
User mobility	low	medium	high
Dispersion (multipath)	none	medium	high
Path loss	low	extended	high
Impact of ambient noise	low	medium	high

impact of ISI, and ambient light, while the Tx-Rx alignment is relaxed and P-t-MP communication is possible.

Table 8.1 summarizes important features of the basic Tx-Rx configurations in OWC. Because in addition to the link type the lighting scenario may also vary while used for VLC, a dynamic data rate adaptation appears necessary, as already proposed in [17] and [18]. Such a feature would enable efficient use of the channel and its instantaneous character, and thus would substantially contribute to making VLC links robust and ready for various use cases. There are several approaches and options based on the fundamental principles of high-speed VLC transmission, which are addressed in this chapter. Thus, we will not dive deeper into the matter of dynamic data rate adaptation. In the following, some illustrative VLC scenarios, mainly using high-speed transmission, are discussed.

Pure wireless broadcast links could provide passenger information, etc., via the general lighting, e.g. on underground stations (Fig. 8.3) or inside the metro cars, where lights are always on anyway. Such indoor systems require unidirectional data transfer (streaming), a few meters transmission reach and a wide FOV, which is inherently given by lighting. The basic functionality of such an application is quite similar to the traditional and most commonly used optical wireless application (at very low speed, but using infrared light), namely the remote control. However, today's technology can provide very high data rates up to the Gbit/s range.

Another example of VLC combined with general lighting, as shown in Fig. 8.4, is also known as optical WiFi or Li-Fi (light fidelity). In wireless local area network (WLAN) scenarios like this, the downlink is provided in the same way as above, while the uplink from the laptop to an access point at the ceiling can be established, e.g. using a LOS infrared (IR) link (see e.g. [19]). Such a system can offer bidirectional communication with wide FOV P-t-MP visible light downlinks at speeds in the range of several Mbit/s or much more depending on the link conditions (LOS or diffuse), and IR directed LOS P-t-P uplinks of a few Mbit/s, assuming both fair Tx-Rx alignment and optical power [20].

Machine-to-machine communication is expected to be a further broad field of VLC application, e.g. with respect to wireless exchange of high data volumes within small and dense communication cells. It is also assumed that in industrial environments there may be harsh electromagnetic conditions going along with the highest demands on security



Figure 8.3 Broadcast of multimedia passenger information by visible light on an underground station.



Figure 8.4 Optical wireless LAN scenario where the downlink is provided by VLC while the uplink is realized, for example, by infrared light.

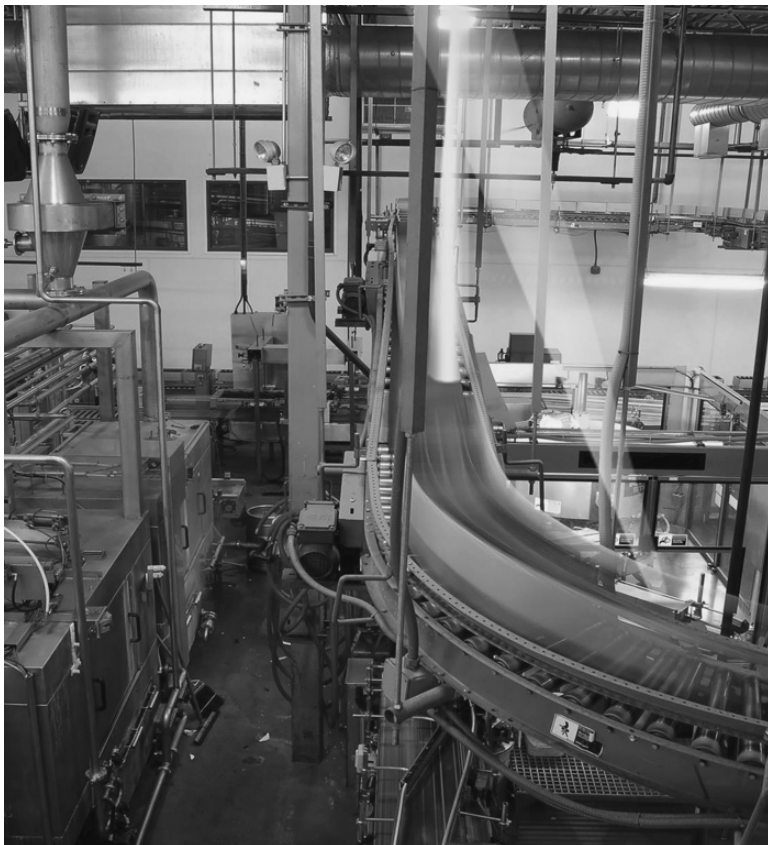


Figure 8.5 Bidirectional VLC applied in a production line, e.g. in order to trigger the device under assembly for performance tests and to receive the results during shift on the conveyor.

and reliability making it difficult or even impossible to use radio-frequency systems. VLC directed LOS links on the other hand could provide suitable high-speed bidirectional links. As an example, Fig. 8.5 illustrates a scenario where performance tests of products under assembly happen while the units are moving on a conveyor, and data exchange with an assessing central server is required at the same time.

8.3 Aspects of high-speed VLC transmission

In particular, when combined with lighting, key enablers for VLC are that the LEDs do not flicker, that only a minimum of extra power is needed, that VLC works at the commonly used brightness levels, and that well-established functions of lighting such as dimming are possible without reservation [13, 14, 21]. These aspects are addressed in Section 8.6.1. From the transmission technology point of view, the LED modulation bandwidth is just as crucial as the wireless channel capacity and how to exploit it efficiently. These subjects will be discussed in the subsequent sections.

8.3.1 LED modulation bandwidth

White light LEDs, as key VLC elements, are manufactured by appropriately adding the light of three or four colored emitters, i.e. red, green and blue (RGB, trichromatic) or red, yellow, green and blue (RYGB, tetrachromatic) LED devices, respectively. As an alternative, a single blue emitter chip coated with a yellowish phosphor layer (YB, dichromatic) is used. The RGB and RYGB white light sources provide the desired spectral output, but are hardware-intensive as multiple LEDs are required. In addition, they tend to render pastel colors unnaturally, a fact which is largely responsible for the poor color-rendering index of RGB white light. As a result, the YB-LEDs are currently the device of choice for illumination, and thus also for low-cost VLC.

While typical RGB and RYGB LEDs created for lighting purposes offer a 3 dB modulation bandwidth of some ten MHz, the bandwidth of YB-LEDs is much lower, i.e. in the order of a few MHz, see e.g. [22, 23]. This is because of the slow temporal response of the yellow phosphor layer. On the other hand, as explained in [24], a bandwidth of several tens of MHz could be expected in the absence of the phosphor layer. Accordingly, it is good practice to place a blue optical filter in front of the PD at the Rx side in order to receive only the blue component of the light and to take advantage of its larger modulation bandwidth [25]. This, however, comes along with a lower power budget and signal-to-noise ratio (SNR), as the major portion of the received light spectrum is filtered out [26]. Alternatively, equalization techniques can be used to combat the influence of the phosphor layer [27, 28]. To cite an example, an array of 16 YB-LEDs was modified in that way to have a bandwidth of 25 MHz without blue filtering [29].

Regarding the LED modulation bandwidth, in a more general sense it is worth mentioning that according to experimental studies the modulation bandwidth of white light as well as of colored LEDs can be exploited far beyond the 3 dB drop. For instance, in [30] a bandwidth of 100 MHz has been used for modulation, while the LED 3 dB bandwidth was about 35 MHz.

Because, in addition to the commonly used (inorganic) LEDs in lighting systems, organic LEDs (OLEDs) also become attractive for replacing large area luminous sources, it should be noted that OLEDs are considered in VLC too. However, they offer an inherently low modulation bandwidth in the range of about 100 kHz [31, 32], and thus they are not in the scope of this chapter.

8.3.2 Channel capacity

As briefly discussed in the context of VLC applications above and summarized qualitatively in Table 8.1, the capacity of the optical wireless channel in a given indoor scenario strongly depends on the presence of both LOS and diffuse signal components. A useful means of describing the channel state by a single parameter is the Rician K -factor, which is defined as the ratio of the (electrical) LOS and diffuse channel gain (loss), i.e. K [dB] = $20 \log(\eta_{\text{LOS}} / \eta_{\text{DIFF}})$. Following the analysis in [33, 34], where an empty model room and realistic parameters are assumed as an example, the frequency response is

calculated and illustrated in Fig. 8.6 (a). The diagram shows the composite channel frequency response magnitude obtained from the analytical model for several illustrative K -factors. Clearly, the channel response highly depends on the LOS prominence (described by the K -factor). Where the LOS is weak or blocked, the response is approximately low-pass and the bandwidth is quite poor. As the LOS gets more pronounced, the channel response varies until it becomes almost flat for sufficiently large K -factors, rendering bandwidths up to an order of magnitude greater than in the diffuse case. The notches in the channel characteristic are due to destructive interference of the two frequency components. Assuming, e.g. a realistic working area hot-spot scenario, the K -factor span of interest is about -20 to $+25$ dB.

The simplest way to obtain reliable connectivity under all channel conditions within the coverage area of a given scenario is to realize a statically designed system, with transmission parameters fixed according to the worst case. However, such a system would not be able to benefit from the channel properties. In order to illustrate the potential of the indoor optical wireless channel, the upper capacity bound in terms of transmission rate for different channel states and two optical power limits ($P_O = 0.1$ and 0.4 W) is presented in Fig. 8.6 (b). For comparison, the curves of a statically designed system, aimed to guarantee a constant transmission performance in the whole area of interest are also shown. From Fig. 8.6 (b) it becomes clear that it is extremely attractive to exploit the channel capacity, in particular at growing K -factors, where the link becomes more and more transparent. The gain (with respect to a worst-case design) grows with the K -factor, and also by increasing the optical transmit power, where it becomes significant even at decreasing values of K . The information rate also depends on the electrical bandwidth, which may be limited by the LED as outlined above in Section 8.3.1.

The calculations were made when the transmit power was allocated as best possible to the subcarriers of a multiple subcarrier modulation (MSM) scheme. In doing so it is also shown in [35] that optimum power allocation gives negligible advance when the electrical bandwidth is limited to about 20 MHz, but offers more improvement at higher bandwidths, particularly for low Tx powers under MSM methods, which are the focus of this chapter. The topic of Tx power dynamic range and its influence on the information rate is analyzed in [36]. It is shown there that a Tx with a wide linear dynamic range of 20 dB or more provides sufficient electrical power for OWC with an optical transmit power close to the boundaries of the dynamic range, where the LED appears to be off or powered close to its maximum. It is also shown there that an average optical power sweep over 50% of the dynamic range can be accommodated using an appropriate modulation scheme, if the information rate is reduced by only $\sim 10\%$.

In addition to the theoretical work discussed above, results of an experimental channel characterization can be found for example in [37], where a VLC channel bandwidth of 63 MHz is reported for a certain room geometry.

The cited work and further results indicate that although the well-known Shannon channel capacity formula for a band-limited, average power-limited additive white Gaussian noise (AWGN) channel cannot be applied directly to the VLC channel, it can

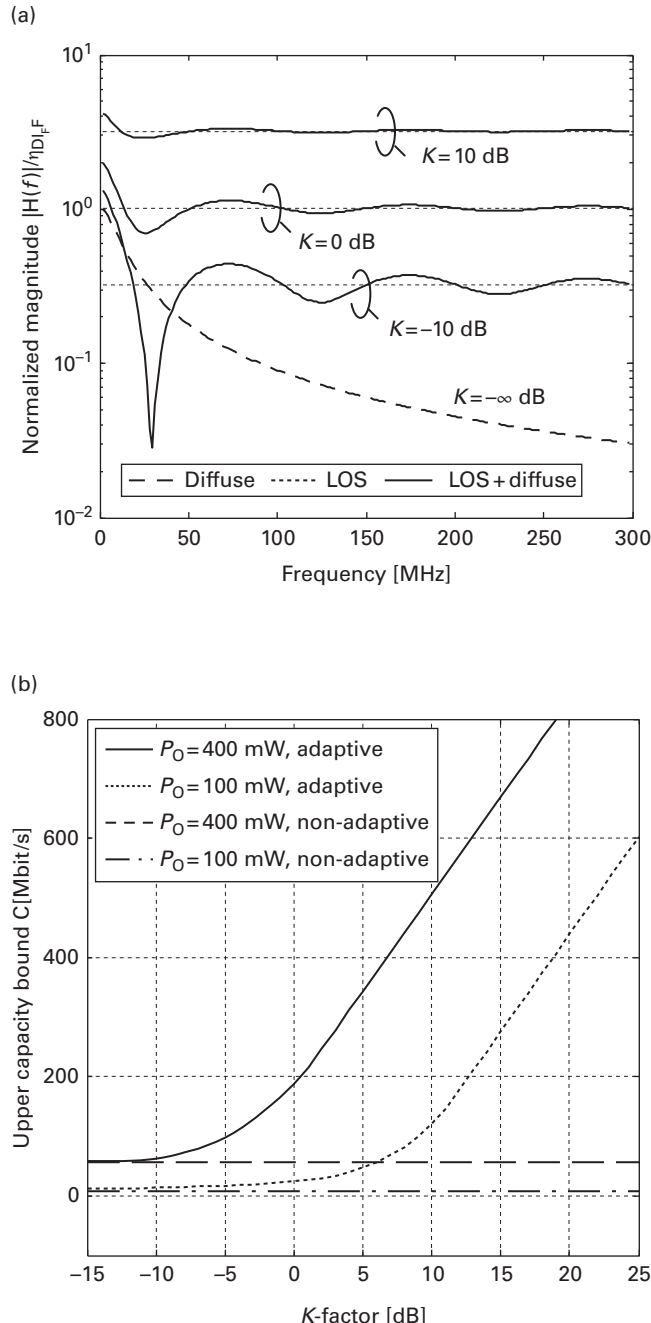


Figure 8.6 (a) Frequency response of the optical wireless channel in a model room for different K -factor values. The derivation is outlined in [33], where $\Delta t = 10 \text{ ns}$ delay between LOS and diffuse signal components is assumed. (b) Upper capacity bound C of an adaptive and a non-adaptive OWC system (bandwidth 100 MHz) as a function of the channel state and the mean optical power P_O as parameter.

be adapted in many cases to find the limit of reliable OWC. As a conclusion, it is noted that in non-diffuse situations the channel presents much more capacity than offered by the LED, depending on the Rician K -factor. This calls for advanced spectrum efficient LED modulation if high-speed communication is desired. In order to maximize the system throughput, while reliable operation and full coverage are maintained, an OWC system could be designed that is bandwidth- and rate-adaptive. Such an adaptive system reduces the data rate under adverse channel conditions until a desired bit error performance is attained. However, such a feature requires a reliable low-speed feedback link for transferring the necessary channel state information from the Rx to the Tx.

8.3.3 Considerations on high-speed LED modulation

With the aim of developing simple and low-cost VLC systems, it is an obvious step to choose simple and well-known modulation formats such as OOK, pulse-width modulation (PWM), or M -ary pulse-amplitude modulation (M -PAM), which can be applied in a straightforward way using intensity modulation and direct detection. The literature provides a lot of proposals and demonstrations on a low-speed level, but also some examples where several 100 Mbit/s have been achieved using OOK, cf. for instance [7, 38]. However, if higher transmission speeds are needed, the above mentioned modulation schemes begin to suffer from the undesired effects of ISI due to the non-flat frequency response of the optical wireless channel [15]. Hence, a more resilient and, in view of the limited LED bandwidth, a more spectrum efficient technique such as MSM is required.

In the VLC transmission chain, the LED device is a major source of non-linear distortion. This is due to a non-linear transfer function within the LED's operating range. As the significance of such behavior strongly depends on the modulation scheme used, non-linearity aspects have been extensively studied in numerous papers, such as [39–43]. The LED non-linearity is of particular importance if spectrally efficient MSM modulation is applied in order to exploit the LED's bandwidth. Using such modulation schemes, which this chapter is focused on, the dynamic range and linearity of the emitter device may severely limit the achievable performance [4]. In order to mitigate such restrictions the selection of a proper modulation format is crucial [44], [45], while the LED operating point has to be defined carefully [46], and signal clipping prior to modulation has to be considered [47].

Beyond the non-linearity issue, further effects on the LED performance, such as LED degradation due to ageing or junction temperature variation have to be considered. First studies on this subject have been published, e.g. in [48], however, further investigations on the LED behavior under VLC operation conditions are necessary.

8.4 DMT modulation and variants

MSM techniques are modulation schemes where information is modulated onto orthogonal subcarriers located in the frequency band considered. The sum of the modulated

Table 8.2 Contrast between typical OFDM systems and optical multimode transmission based on intensity modulation and direct detection.

Area of application	Typical example	Carrier of information	Type of detection	Special receiver requirement
Electrical OFDM transmission	Radio transmission, e.g. WiFi, DVB-T	Electrical field	Coherent	Local oscillator
Optical OFDM transmission	Long-haul high-speed single mode fiber (SMF) links	Optical field	Coherent (only one optical mode)	Local oscillator
Optical IM/DD transmission	Multi-mode fiber (MMF, POF) links, OWC	Optical intensity	Direct (multiple optical modes)	None

subcarriers is then modulated onto the instantaneous power of the transmitter. Usually MSM is implemented by *orthogonal frequency division multiplexing* (OFDM), which has been widely employed in both wired and wireless digital communications. Applications of the basic OFDM principle include WLAN and terrestrial digital video broadcasting (DVB-T), as well as digital subscriber line systems (xDSL) and power line communication (PLC), where a baseband version of OFDM, better known as *discrete multitone* (DMT) modulation is used. Due to the capability to mitigate ISI, and other advantages including the ability to adapt easily to different channels, MSM was also considered for OWC [49].

Conventional systems such as WLAN or DVB-T use coherent transmission, where the signals are in general complex and bipolar. The same applies to laser-based long-haul optical transmission systems using single-mode fibers. Concerning *optical multimode transmission* as in VLC, it is, however, extremely difficult to collect substantial signal power at the Rx in a single electromagnetic mode. In the final analysis, this means that *intensity modulation with direct detection* (IM/DD), as also used for instance in OOK and PWM-based systems, has to be considered as the only practicable transmission method. Thus, only the light intensity (and not the phase) represents the information to be transmitted, i.e., the transmitted signal is of real and non-negative (unipolar) value. At the receiving end, a photodetector produces an electrical current proportional to the received power, and accordingly proportional to the square of the received electrical field [16]. The differences between traditional OFDM transmission using coherent detection and IM/DD systems are briefly summarized in Table 8.2.

In consequence of IM/DD transmission, the conventional OFDM modulation scheme cannot be directly applied in optical multimode systems. Therefore, researchers have devoted significant efforts to designing OFDM-based modulation schemes, which are purely unipolar. Using OFDM in VLC was first proposed by Tanaka *et al.*, and their basic studies can be found in [50].

The task to create a unipolar signal for transmission is commonly solved by adding a DC bias to the bipolar OFDM signal [18, 25]. We call this scheme *DC-biased DMT*, however, it is also known as DC-biased OFDM and DC-clipped OFDM. Another method

clips the entire negative excursion of the OFDM waveform. Impairments from clipping noise are avoided by appropriately choosing the subcarrier frequencies for modulation. This technique is called *asymmetrically clipped optical OFDM* (ACO-OFDM) [51]. A third method also clips the entire negative signal excursion, but modulates only the imaginary parts of the subcarriers such that the clipping noise becomes orthogonal to the desired signal. This technique is well-known as *pulse-amplitude-modulated discrete multitone modulation* (PAM-DMT) [52]. These modulation schemes and their properties when applied to VLC are discussed in the subsequent sections.

8.4.1 DC-biased DMT

DMT as a baseband version of OFDM modulation is a key technique used on slowly time-varying two-way channels, e.g. in copper-based xDSL and PLC systems. It is important to know that DMT is also of relevance for low-cost short-range optical transmission using multimode silica fibers and plastic optical fibers [52, 53]. Usually, modulation onto multiple subcarriers of different frequencies for simultaneous transmission, as well as demodulation, are based on discrete Fourier transformation (DFT) [54, 55]. Thus, inverse fast Fourier transform (IFFT) and fast Fourier transform (FFT) are the main building blocks of the Tx and Rx, respectively.

On the Tx side, first of all the serial data stream is partitioned into multiple parallel streams of lower data rates, typically followed by mapping to a quadrature amplitude modulation (QAM) constellation, as illustrated in Fig. 8.7. A straightforward way to obtain real-valued time domain signals, as required in LED-based VLC, is to use the well-known property that the N -DFT of a real-valued sequence has conjugated symmetric coefficients around the point $N / 2$ [56]. This means that by enforcing conjugate symmetry (often referred to as *Hermitian symmetry*) on the IFFT input vector \mathbf{X} in the frequency domain, a real-valued time domain signal can be directly obtained at the output of the IFFT block.

Following this approach, with $N / 2$ (actually $(N / 2) - 1$) independent subcarriers envisaged in the system to carry information, an N -IFFT block is required to generate a real-valued OFDM/DMT symbol. According to the Cooley–Tukey algorithm [56], the complexity of the FFT operation scales with $N \log_2 N$. Hence, as a moderate number of subcarriers is considered in optical wireless systems, the size of the DFT blocks is not an implementation issue. On the other hand, DFT enables digital implementation of DMT modulation without prohibitive analog filter banks.

The IFFT input vector $\mathbf{X} = [X_0 \ X_1 \ \cdots \ X_{N-1}]^T$ consists of the data to be transmitted (elements $X_1, X_2, \dots, X_{(N/2)-1}$) and the further elements defined according to the Hermitian symmetry constraint as

$$X_n = X_{N-n}^*, \text{ for } 0 < n < N/2, \quad X_0 \in \mathbb{R}, \quad X_{N/2} = 0. \quad (8.1)$$

The first input X_0 , corresponding to zero frequency, must be real-valued and is generally left unmodulated. It can be set to zero or alternatively to the DC level of the output signal (see below).

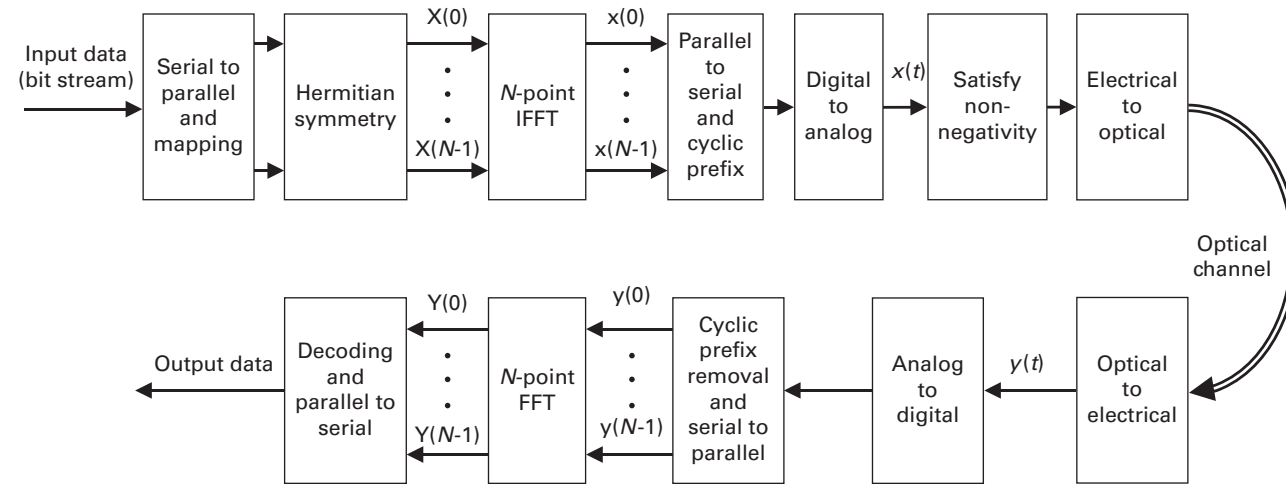


Figure 8.7 Building blocks of DMT-based transmission over an optical IM/DD channel. Note that the tasks of satisfying non-negativity and digital-to-analog conversion may be swapped depending on the hardware implementation of the DC biasing.

After creation of the input vector, $[X]$ is fed into the N -point IFFT block, as shown in Fig. 8.7. Assuming data symbols of complex-valued modulation formats (usually M -QAM), where the input vector elements appear in the form $X_n = a_n + jb_n$, the time samples at the N -IFFT output are

$$\begin{aligned}
 x(k) &= \frac{1}{N} \sum_{n=0}^{N-1} X_n e^{j2\pi nk/N} = \frac{X_0}{N} + \frac{1}{N} \sum_{n=1}^{(N/2)-1} X_n e^{j2\pi nk/N} + \frac{1}{N} \sum_{n=1}^{(N/2)-1} X_n^* e^{-j2\pi nk/N} \\
 &= \frac{X_0}{N} + \frac{1}{N/2} \sum_{n=1}^{(N/2)-1} \Re\{X_n e^{j2\pi nk/N}\} \\
 &= \frac{X_0}{N} + \frac{1}{N/2} \sum_{n=1}^{(N/2)-1} a_n \cos(2\pi nk/N) - b_n \sin(2\pi nk/N) \\
 &= \frac{X_0}{N} + \frac{1}{N/2} \sum_{n=1}^{(N/2)-1} \sqrt{a_n^2 + b_n^2} \cos\left(2\pi nk/N + \arctan(b_n/a_n)\right), \quad (8.2)
 \end{aligned}$$

where $k = 0, 1, \dots, N - 1$ denotes the index of the time domain sample. Apart from the conjugate-symmetry property of the input vector given by Eq. (8.1), the symmetry property of the DFT twiddle factors $e^{j2\pi(N-k)k/N} = e^{-j2\pi N k / N}$ has also been exploited in Eq. (8.2). Obviously, a sum of $(N/2) - 1$ sampled real-valued cosinusoids is obtained at the IFFT output.

In order to mitigate effects of the multipath channel and to avoid ISI, OFDM and DMT use a guard interval, which is placed between the transmitted symbols (blocks) in the time domain. This guard band is formed simply by taking a number of L samples from the end of each symbol, and copying them as its prefix, as shown in Fig. 8.8. It is hence referred to as *cyclic prefix* (CP). This $(M + L)$ -point sequence corresponds to the samples of the multicarrier DMT time-discrete sequence to be transmitted, which is referred to as a DMT symbol.

In order to receive and properly demodulate the DMT symbols, two conditions have to be satisfied. Firstly, the length of the DMT symbol without CP should be longer than or equal to the duration of channel impulse response $h(t)$ in order to avoid ISI. Additionally, the CP length should be chosen so that its duration is longer than or equal to the delay

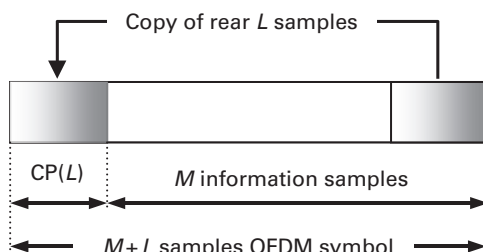


Figure 8.8 Generation of the cyclic prefix guard interval and structure of a DMT symbol. CP: cyclic prefix.

spread of $h(t)$. Although the CP introduces some redundancy, and thus reduces the overall data rate, it eliminates both ISI and inter-carrier interference from the received signal and is the key to simple equalization in OFDM [55].

When assuming a limited signal bandwidth B in the baseband, which is divided among $N/2$ independent subcarriers, the subcarrier spacing is $\Delta f = 2B/N$, while the frequencies in the N -IFFT block cover the bandwidth of $2B$ because of the Hermitian symmetry constraint. The period of a DMT symbol, containing N time samples, is $T_{\text{FFT}} = 1/\Delta f$, which leads to the sample interval $T_{\text{sam}} = 1/2B$ in the time domain. According to the sampling theorem, this is sufficient to completely determine the continuous signal at the output of the digital-to-analog (D/A) converter. As the CP of length $T_{\text{CP}} = LT_{\text{sam}}$ has to be added after the IFFT, the actual duration of the real-valued DMT symbol is $T_{\text{DMT}} = T_{\text{CP}} + T_{\text{FFT}}$. Considering in addition Eq. (8.2) and the identity

$$2\pi \frac{n k}{N} = 2\pi n \frac{2B}{N} \frac{k}{2B} = 2\pi n \Delta f k T_{\text{sam}} = 2\pi f_n t_k, \quad (8.3)$$

where $f_n = n\Delta f$, $n = 1, 2, \dots, N-1$ and $t_k = kT_{\text{sam}}$ for $k = 0, 1, \dots, N-1$, the continuous-time signal after D/A conversion can be expressed as

$$x(t) = \frac{X_0}{N} + \frac{1}{N/2} \sum_{n=1}^{(N/2)-1} A_n \cos(2\pi f_n t + \varphi_n), \quad -T_{\text{CP}} \leq t < T_{\text{FFT}}. \quad (8.4)$$

In this expression, $A_n = \sqrt{a_n^2 + b_n^2}$ and $\varphi_n = \arctan(b_n/a_n)$ are the amplitude and the initial phase of each cosinusoid on the frequency occupied by the n th subcarrier, determined by the amplitude and phase of the complex-valued symbol X_n at the corresponding IFFT input. Note that the signal $x(t)$ could also be obtained with a bank of $(N/2)-1$ analog filters. After D/A conversion, an analog low-pass filter is implemented to suppress the aliasing spectra. At the same time, this filter performs interpolation of the discrete signal waveform.

Figures 8.9 and 8.10 illustrate an example of the signals at the input and output of the DMT modulator. In this example, three out of $N=16$ orthogonal carriers in a bandwidth of $B=20$ MHz are modulated by 16-QAM to generate an input vector $[X] = [0, (1+j), (3-j), 0, (-3+3j), 0, 0, 0]^T$ (before Hermitian symmetry enforcement). The input of the 16-IFFT block is shown in Fig. 8.9, while the contributions of individual subcarriers at the output as well as the resulting output signal are illustrated in Fig. 8.10 (a)–(c) and (d) respectively.

If the bias was not introduced directly at the system input by setting X_0 appropriately, i.e., if $X_0 = 0$ was chosen, non-negativity of the transmit signal $x(t)$ has to be achieved after D/A conversion. A very common and simple method is to add a fixed DC bias to the bipolar DMT signal, as illustrated in Fig. 8.10 (e), cf. for instance [25, 49, 52, 57]. The required DC bias is equal to the maximum negative amplitude of the DMT signal. Owing to the high PAPR of DMT signals, a bias of at least twice the standard deviation of the bipolar DMT signal distribution is required to minimize clipping [58]. Any remaining negative values would be clipped, which also applies to positive peaks upon exceeding the limiting amplitude. Such symmetrical or asymmetrical clipping

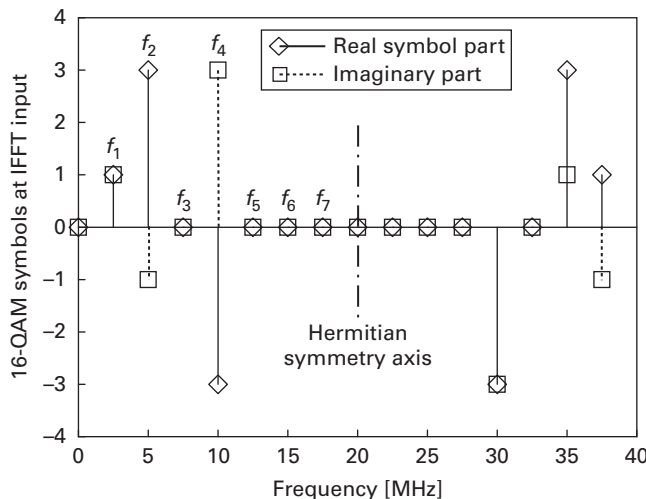


Figure 8.9 Example of 16-QAM symbols on individual subcarriers in f -domain at the IFFT input according to the input vector $\mathbf{X} = [0, (1+j), (3-j), 0, (-3+3j), 0, 0, 0]^T$ before Hermitian symmetry enforcement. Further parameters are $N = 16$, $B = 20$ MHz, and $L = 2$.

introduces clipping noise and thus affects transmission. In practice, controlled clipping of high negative peaks in front of the optical source is often permitted, given an unlikely occurrence in a DMT signal. Then, as long as the effect of clipping on the link performance is tolerable, the required DC component can be reduced to a certain extent [33], cf. also Section 8.6.1. An optimal DC bias of a symmetrically clipped signal can be inferred, e.g. from [59, 60]. It is shown there that iterative decoding with clipping noise estimation and subtraction can reduce the bit error ratio (BER) at the expense of an increased computational complexity.

Returning to Fig. 8.7, the signal reaches the Rx after undergoing the influences of the time-dispersive channel and ambient light as the dominant source of noise in the channel. A simple (low-cost) photodetector is used to convert the IM signal to an electrical signal, while the bias component is discarded by AC-coupling. After analog-to-digital (A/D) conversion, the CP is removed and N -point FFT processing is performed. Thanks to the preserved orthogonality, the subcarriers can be processed separately. In principle, only the outputs $n = 1, 2, \dots, (N/2) - 1$ need to be further regarded, since they are the ones carrying information. Because the frequency response over the subcarrier bandwidth can be considered as flat fading, the signal is usually equalized simply by means of a single-tap linear feed-forward equalizer with zero forcing or minimum mean squared error (MMSE) criteria before decoding.

Adding the DC bias at the Tx results in extra power consumption to an equivalent extent. If the light source is used at the same time for illumination, this amount of power fulfills its purpose with respect to lighting and is thus not wasted. Only if illumination is not required, such as in the uplink of a Li-Fi system, the DC bias can significantly jeopardize energy efficiency [15].

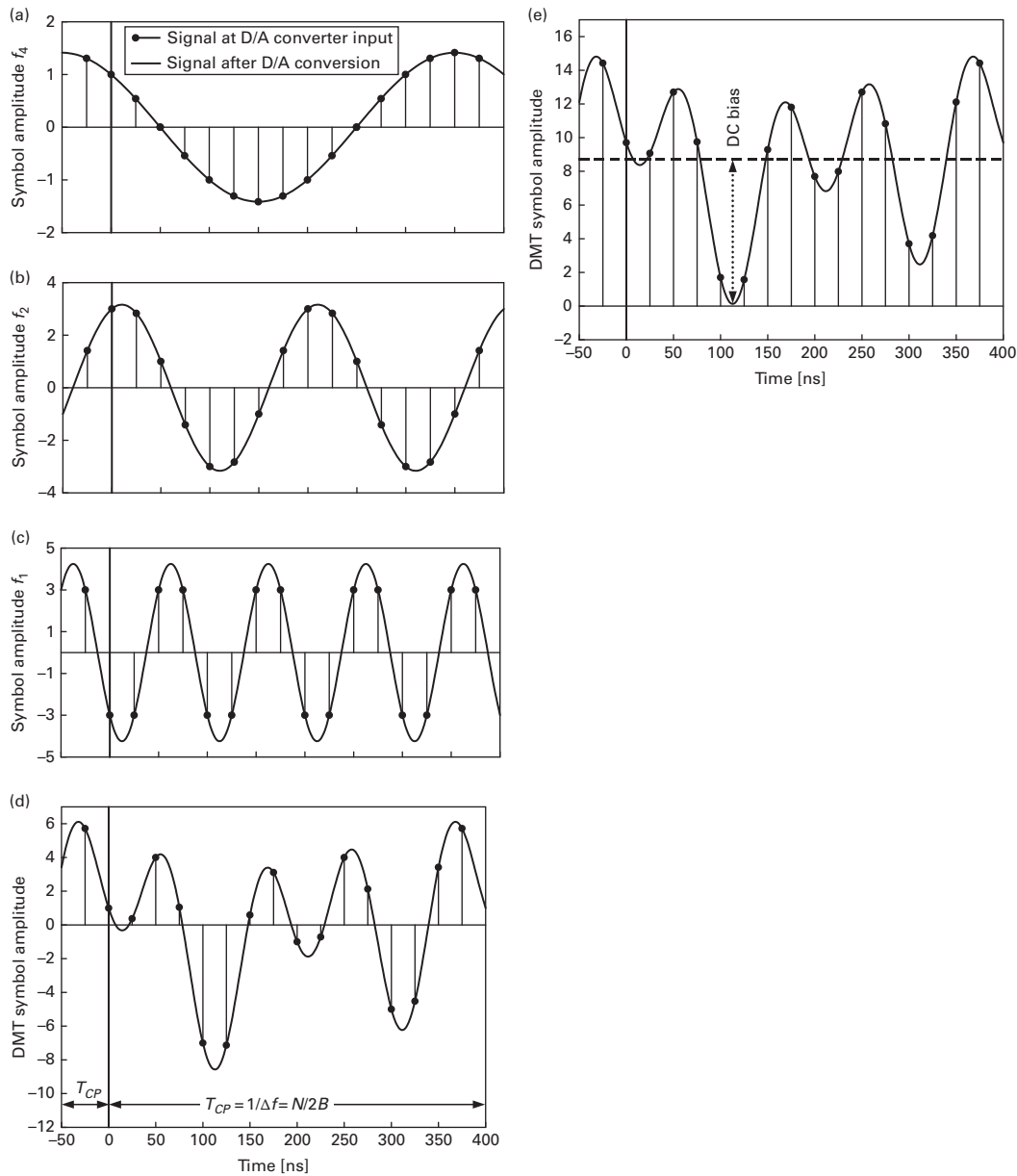


Figure 8.10 (a)–(c) The individual contributions of modulated subcarriers; (d) the DMT symbol in the t -domain. Both sampled and continuous signals before and after D/A conversion are shown. Note that the amplitudes are scaled by N to achieve the same level as in the f -domain. In this example, the real-valued bipolar DMT signal with $N = 16$ subcarriers used in the example (d) is made unipolar by adding an appropriate DC bias (e).

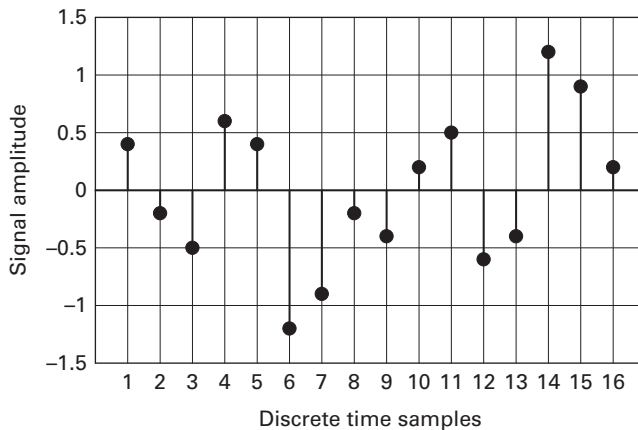


Figure 8.11 Example of an ACO-OFDM time domain signal with $N = 16$ subcarriers (the CP is not considered here). The positive and negative parts of the waveform are anti-symmetrical along the zero-axis. Thus, hard-clipping the negative values at the zero level only will discard redundant information.

8.4.2 Asymmetrically clipped optical OFDM (ACO-OFDM)

The main objective of improving the preparation of OFDM signals for IM/DD transmission is to reduce the DC bias, which is indispensable in the DC-biased DMT scheme, to a minimum value. Note that the LED turn-on voltage in fact defines the lower bound of the bias. For the sake of simplicity this parameter is neglected in the following. Approaches for improving the power efficiency are driven by the basic aim to create a real-valued bipolar time domain signal, where the entire information is present at least in the positive parts. This would enable simply clipping the negative parts of the signal when modulating the optical source. The main embodiment of such asymmetric clipping is the method of ACO-OFDM introduced by Armstrong *et al.* [51, 58].

While the basic function blocks are the same as in DC-biased DMT, the ACO-OFDM scheme exploits the properties of Fourier transform by introducing a constraint on the subcarriers used for modulation, i.e., only odd-numbered subcarriers are used whereas the even subcarriers are set to zero. Considering again Hermitian symmetry, up to $N/4$ subcarriers (CP included) are used for modulation [51, 61]. As illustrated in Fig. 8.11, the IFFT output presents time samples along the zero-axis, where the negative part is an anti-symmetrical copy of the positive part. Finally, this means that the information of both parts is the same. For that reason, clipping of the negative part will provide a unipolar signal without any loss of information. Related proofs can be found in [43, 51].

Insertion of a CP and D/A conversion is done in the same way as in the case of DC-biased DMT. Subsequently, the unipolar signal is used for modulating the LED.

The idea of using only the odd-numbered subcarriers for data transmission includes the fact that all of the intermodulation products resulting from the asymmetric clipping are orthogonal to the data, i.e., clipping distortion falls on the unused even-numbered subcarriers and does not affect the odd-numbered ones. Even though the effect of

clipping does not result in inter-carrier interference on the data-carrying odd subcarriers, it reduces all their amplitudes by half [51, 58, 62]. Moreover, the restriction to use only odd-numbered subcarriers can degrade performance in a frequency-selective channel. Particularly when bit and power loading is employed, where the allocation of bits and power per subcarrier is adapted to the SNR of the frequency-selective channel [54, 63], the subcarrier constraint will result in a non-optimal adaptation to the channel response and thus in an unfavorable system performance. This calls for carefully controlled and effectively compensated solutions [64], in particular if the number of subcarriers is small.

At the Rx, the PD detects the transmitted intensity and the analog signal is converted into a digital one. It is well-known that OFDM systems are highly sensitive to synchronization errors. Due to the fundamentally different waveforms in ACO-OFDM and traditional OFDM systems, conventional synchronization could fail if applied directly. A technique tailored to the ACO-OFDM scheme using an appropriate training sequence is presented in [65]. According to [66], the loss of bandwidth efficiency associated with a training sequence can be avoided in systems employing ACO-OFDM if the CP-based method is replaced by the presented technique of low-complexity blind timing synchronization.

In conclusion, ACO-OFDM has a significantly lower detrimental DC component compared to DC-biased DMT. Thus, the modulation scheme is highly power efficient, but at the expense of exploiting only half of the subcarriers for data transmission.

8.4.3

Pulse-amplitude-modulated discrete multitone (PAM-DMT)

The concept of pulse-amplitude-modulated DMT (PAM-DMT) introduced in [52] also aims at asymmetric clipping at zero value and transmission of only the positive parts of the DMT signal as in ACO-OFDM. This means that again anti-symmetry of the time domain signal is needed after IFFT.

Firstly, as in DC-biased DMT and ACO-OFDM, Hermitian symmetry is induced in order to achieve real-valued signals in the time domain. However, only the imaginary components of the PAM input signal are used further, while the real components are set to zero. The IFFT then presents real-valued time domain samples that exhibit anti-symmetry, as desired. Similarly to DC-biased DMT, up to $N/2$ subcarriers (including CP) are used, i.e. the elements $(X_1, X_2, \dots, X_{(N/2)-1})$ of $[\mathbf{X}]$ carry the imaginary PAM signal components, while $X_0 = 0$. After CP insertion and along with D/A conversion, the entire negative excursion of the electrical waveform is clipped without any loss of information, and is then used for driving the LED.

In [52] it is shown that the distortion resulting from asymmetric clipping falls orthogonally onto the real-valued parts of the PAM signal, without influencing the imaginary parts modulated with information, and thus without affecting the system performance. Proofs of anti-symmetry and the property of the clipping distortion terms can be found in [43]. At the Rx, demodulation and decoding the data are performed straightforwardly and similarly to the schemes discussed before.

In conclusion, PAM-DMT uses all subcarriers as in the DC-biased DMT scheme, but the modulation is restricted to just one dimension. Hence, PAM-DMT has the same spectral efficiency as ACO-OFDM. Regarding the power efficiency, the PAM-DMT characteristics are similar to those of the ACO-OFDM scheme.

8.4.4 DMT/OFDM performance and mitigation of disruptive effects

Numerous analytical studies on characteristics of the modulation schemes described above and on differences in their performance in VLC have been published in recent years. The most important items are discussed in this section.

If reduction of the high PAPR is required, simple non-linear techniques can be applied, possibly in combination with some form of predistortion [55, 67]. Various precoding techniques for PAPR reduction in asymmetrical clipped systems such as ACO-OFDM and PAM-DMT are analyzed in [68]. It was shown there that precoding with small effort could gain PAPR reduction of about 3 dB, making this technique attractive for PAPR reduction in systems with asymmetrical clipping.

Several comparative analyses have been performed including mathematical description of effects and simulations under various conditions, cf. in particular [69–73]. To shed light on one of the results, it was found that ACO-OFDM and PAM-DMT have virtually identical performance at different bit rates and spectral efficiencies, as demonstrated in the study [70], and is also indicated in several other publications. This is because in ACO-OFDM, half of the subcarriers are filled, but in PAM-DMT half of the quadrature is filled. Therefore, the same performance is obtained when a flat frequency response is considered.

In practice, clipping the LED modulation signal clearly affects the system performance. The modulation order and other parameters of relevance such as the bias level (including the LED turn-on threshold) are therefore of high significance. While AWGN is the main type of noise in the case of low SNR, clipping distortion dominates at large SNR values. Thus, LED clipping effects have to be considered and the modulation order as well as the power of the transmit signal should be optimized. Methods for optimization are given e.g. in [45]. Another analytical study on the trade-off between biasing and clipping suggests that rather than eliminating all clippings, the SNR is in fact optimal with some deliberately introduced non-linear clipping distortion because of higher power efficiency at a lower bias level. A corresponding biasing strategy is proposed in [74]. This method does not require any on-line calculation and can be used in different optical channels with different Rx figures and modulation schemes; however, an uplink between Rx and Tx is necessary.

Besides asymmetric clipping to achieve non-negativity, the signal for LED modulation often has to be double-sided clipped in order to fit into the linear range of the LED [45, 73]. This introduces non-linear distortions. In a more advanced approach scaling of the transmit signal is proposed in order to accommodate the large PAPR in the LED's linear range and to adapt the DC bias accordingly. More precisely, such signal shaping as presented in [71] conditions the transmit signal to meet the optical power constraints of the Tx by means of scaling (realized by digital signal processing, DSP) and by DC biasing (realized in the analog Tx circuitry). An optimal signal shaping enables the Gaussian transmission signals to minimize the electrical SNR requirement. As in the case

Table 8.3 Computational complexity needed for the three modulation schemes at low (upper three rows) and high (lower three rows) electrical bandwidth, expressed in terms of real operations per bit. For parameters in detail, cf. [70].

Bit rate (Mbit/s)	Electrical bandwidth (MHz)	DC-biased DMT		ACO-OFDM		PAM-DMT	
		Tx	Rx	Tx	Rx	Tx	Rx
50	25	43.0	45.9	48.5	50.0	48.5	51.5
100	50	43.0	45.9	48.5	50.0	48.5	51.5
300	150	42.4	45.3	48.1	49.6	48.1	51.1
50	50	86.1	91.9	97.0	100.0	97.0	102.9
100	100	85.4	91.2	96.7	99.6	96.7	102.6
300	300	95.3	101.1	106.5	109.4	106.5	112.4

of double-sided clipping, shaping of the Gaussian time domain signals in ACO-OFDM and DC-biased DMT results in a non-linear signal distortion, which is precisely analyzed in [75]. This analysis can be used to translate the signal scaling and DC biasing for a given dynamic range of the LED into electrical SNR, and therefore to BER performance.

As a summary of the numerous analyses and comparisons, both modulation formats using asymmetrical clipping, i.e., ACO-OFDM and PAM-DMT, are best at low spectral and high power efficiency [69, 70, 72]. It is also important to note that multipath dispersion could break the symmetry at the zero line for both of these schemes [52]. Since the symbol period usually by far exceeds the value of dispersion, this effect should not represent a serious issue; however, it has to be confirmed by practical experience. If modulation at higher spectral efficiency is needed, DC-biased DMT performs closer to ACO-OFDM. This is because the clipping noise penalty for DC-biased DMT becomes less significant than the penalty for the larger constellations required if otherwise the ACO-OFDM or the PAM-DMT scheme is used. Thus, DC-biased DMT is expected to deliver the highest throughput in applications where the additional DC bias power required to create a non-negative signal does not matter or can serve a complementary functionality, such as illumination. It should be mentioned that the underlying comparisons typically assume a perfectly compensated LED non-linearity, e.g. using a suitable predistortion. Hence, practical verification is also necessary in that respect.

Beyond performance aspects, the computational complexity of the modulation schemes discussed is of importance. A comparative study on the computational complexity can be found in [70]. The same number of actually used subcarriers in DC-biased DMT and ACO-OFDM was chosen there in order to make a fair comparison. For PAM-DMT, since only one dimension is used to transmit data, the number of subcarriers used was twice that for the other schemes. In other words, from the DFT point of view, the DFT size of the DC-biased DMT scheme is half that of the further schemes.

Table 8.3 summarizes the computational effort needed in the three cases at different bit rates and electrical modulation bandwidths. As can be seen, the complexity of ACO-OFDM and PAM-DMT is nearly the same, while DC-biased DMT has the lowest computational complexity among the three formats, due to the smaller DFT size.

Theoretical work such as mathematical analyses and simulations including ray tracing has to be verified and complemented by experiments under conditions close to reality. At this stage of development in the case of modulation schemes such as DMT, there is the difficulty of time-consuming hardware implementation including DSP algorithms. As an alternative, the widely recognized method of off-line processing (see also Section 8.6.2) is used in nearly all cases published so far. However, this comes along with restrictions, such as focusing on rudimentary or special functions in VLC transmission. For example, the mitigation of background optical noise produced by ambient AC-powered LED lamps or fluorescent light sources was investigated in an experimental VLC setup using off-line processed DC-biased DMT, as reported in [76]. The results have shown that the noise produced by AC-powered LEDs has a negligible effect, as the lowest-frequency subcarrier is far above the 50 or 60 Hz effects, while the noise from fluorescent lamps can be removed by excluding the impaired subcarriers. Moreover, the mitigation of phosphor layer effects caused by the YB-LED-based Tx using channel estimation and one-tap equalization at the Rx was confirmed. Further examples of such experimental work based on off-line processing and mainly targeting high bit rates in a laboratory environment can be found in [8–10, 77–79]. However, more complex subjects including the influence of channel variations and adaptive bit rate link control are hard to investigate under real-time conditions using off-line experiments. If restrictions in DSP speed and bandwidth are accepted, a simple alternative may be to employ programmable hardware such as a DSP development kit. An example of that kind is presented in [40], where it was the aim to investigate the performance of DC-biased DMT transmission in the presence of (infrared) LED non-linearity via a hardware demonstrator including real-time implementation of the digital signal processing.

8.5

Performance enhancement of DMT modulation

In recent years, numerous approaches have been reported aiming at performance enhancement of the discussed modulation schemes, in terms of spectral efficiency and power efficiency as well as PAPR. In the following, a brief overview is given.

8.5.1

Combination of ACO-OFDM and DC-biased DMT modulation

It seems rather obvious to combine the ACO-OFDM modulation scheme, which only uses the odd subcarriers, with a complementary scheme in order to utilize the even subcarriers too. Such an approach, called *asymmetrically clipped DC-biased* optical OFDM (ADO-OFDM) is presented in [80]. In this technique, the odd subcarriers are modulated using ACO-OFDM while the even ones are modulated using DC-biased DMT. The DMT component does not cause interference on the odd frequency subcarriers. Hence, a conventional receiver can demodulate the ACO-OFDM component after detection. On the other hand, the ACO-OFDM signal causes clipping noise, which affects the even subcarriers. This interference can be estimated at the Rx, and thus cancelled at the expense of a 3 dB

noise penalty in the DC-biased DMT component. Clearly, ADO-OFDM provides better bandwidth efficiency than ACO-OFDM, since all subcarriers are used to carry data. Simulation results for an AWGN channel have shown that this method can also achieve better optical power performance than the conventional OFDM schemes [72].

8.5.2 Spectrally factorized OFDM

Another means for improving the optical efficiency of OFDM for IM/DD transmission has been proposed in [81]. The formalism for non-negative multiple subcarrier modulation described there is denoted as *spectrally factorized* optical OFDM (SFO-OFDM). Instead of sending data directly on the subcarriers, the autocorrelation of the complex data sequence is performed in this scheme, which guarantees non-negativity without explicit bias. SFO-OFDM covers all band-limited OFDM signals, and unlike ACO-OFDM, it uses the entire available bandwidth for data modulation. Moreover, it mitigates the high PAPR, which is typical in PAM-DMT and ACO-OFDM systems. According to [81], 0.5 dB in optical power is gained over ACO-OFDM at a BER of 10^{-5} .

8.5.3 Flip-OFDM

A further unipolar modulation approach is known as flip-OFDM [82]. In *flip-OFDM*, the positive and negative parts are extracted from the real bipolar OFDM time domain signal, and transmitted in two consecutive OFDM symbols. Since the negative part is flipped before transmission, both subframes have positive samples, as required in IM/DD systems. The basic flip-OFDM scheme, as presented in [83], performs a compression of the time samples in order to sustain the duration of the original bipolar symbol frame. Consequently, bandwidth and data rate are doubled, while the length of the CP is reduced by 50% when compared to ACO-OFDM. As an alternative, the parameters of an ACO-OFDM system can be maintained by omitting the (not imperatively required) compression of the OFDM subframes. In that way, it has been shown by simulation that both the ACO- and flip-OFDM schemes have the same spectral efficiency and BER performance in the electrical domain. However, flip-OFDM offers savings of 50% in computational receiver complexity over the ACO-OFDM scheme, in particular for slow fading channels [82].

8.5.4 Unipolar OFDM

The so-called *unipolar* OFDM modulation scheme (U-OFDM) has been developed with the aim of reducing the PAPR and to close the 3 dB gap between OFDM and ACO-OFDM for bipolar signals, whilst generating a unipolar signal, which does not require the biasing of DC-biased DMT [84]. The modulation process of U-OFDM starts with conventional modulation of an OFDM signal. After obtaining a real bipolar signal, it is transformed into a unipolar one by encoding the absolute value of each time sample and its polarity into a pair of new time samples (absolute value on one out of two possible

positions depending on the polarity). At the Rx, reconstruction of the original bipolar OFDM signal is straightforward and the process continues with conventional demodulation of an OFDM signal.

Since each time sample from the original OFDM signal is encoded into a sample pair of the U-OFDM signal, the spectral efficiency is the same as of ACO-OFDM, but U-OFDM has better power efficiency in an AWGN channel.

8.5.5 Position modulating OFDM

Based on how the symbols are assigned to the subcarriers, the unipolar operation forms unipolar optical OFDM symbols such as the various operations used to generate the ACO-OFDM, the flip-OFDM, the U-OFDM (see above), or the so-called *position modulation* OFDM (PM-OFDM) described in [85]. PM-OFDM utilizes the DFT approach but removes the Hermitian symmetry constraint. This is done at the Tx by splitting the IFFT output signal corresponding to its real and imaginary components. Their positive and negative parts are further separated, and the two negative signals are flipped by polarity inversion. The resulting four real and positive signals are then sequentially transmitted. Based on this Tx technique, two Rx structures are presented in [85] targeting either high BER performance or low Rx-complexity.

In both, LOS and diffused channels the low-complexity Rx (including time domain MMSE equalizer) achieves the same BER performance as an ACO- or flip-OFDM system, while the total system complexity is significantly lower. On the other hand, the high-performance Rx includes a frequency domain MMSE equalizer and thus an extra FFT and IFFT block, resulting in a marginally higher overall transceiver complexity compared to an ACO-OFDM system. As outlined in [85], this extra effort yields ~ 4 dB improvement at a BER of 10^{-4} in a diffuse optical wireless channel.

8.5.6 Diversity-combined OFDM

When only the odd subchannels are loaded as in ACO-OFDM modulation, the clipping distortion falls exclusively onto the even subchannels, as mentioned above. This natural separation of signal and distortion indicates that at the Rx side, some extent of spectral diversity among even and odd subchannels can be observed. Based on this fact, the idea of an *asymmetrically clipped, diversity-combined* OFDM (AC/DC-OFDM) system has been presented in [86]. There it is revealed theoretically and by simulation, that the effective SNR at the Rx of an ACO-OFDM system can be improved significantly at the expense of one additional IFFT-FFT pair and a diversity combining decoding algorithm at the Rx. As diversity combining adds two different signal components, while an additional noise cancellation would reduce the noise at the Rx, it might be expected that combining these techniques could give further performance gains. This is, however, not true as was shown analytically in [87]. On the other hand, it is important to note that noise cancellation giving a maximum improvement of 3 dB is more computationally efficient than diversity combining.

8.5.7

Further approaches

In order to enhance the overall performance of VLC systems and to efficiently exploit spectrum resources by means of MSM, various additional proposals have been published. Two of them are briefly addressed in this section.

Multicarrier code division multiple access (MC-CDMA) is a transmission scheme that combines the robustness of orthogonal modulation and the flexibility of CDMA schemes. In MC-CDMA, an individual user's complex-valued data symbol is spread over OFDM subcarriers in the frequency domain using a spreading code. The symbols from different users are aggregated in the frequency domain and passed to the OFDM modulator for transformation into the time domain. The further steps of modulation and IM/DD transmission are the same as in the case of DC-biased DMT. At the Rx side, CP removal, FFT, and de-spreading are carried out, respectively. In [88], an optimized selection of active subcarriers is proposed in order to significantly increase the power efficiency in a multi-user indoor scenario. The average transmit power reduction is accomplished by selecting the subcarriers based on pre- or post-equalization, while proper setting of a fixed DC bias ensures low system complexity.

A hybrid *multi-layer modulation* (MLM) scheme designed for optical OFDM-based IM/DD transmission is introduced in [89]. In optical systems, MLM is expected to be capable of offering a fine granularity in terms of throughput versus robustness. Both the concept of MLM and related double turbo Rx algorithms are detailed in this publication. In addition, the layer-specific optimum weights that the MLM scheme should obey are conceived. Significant gains are demonstrated by comparing the MLM-aided technique to the ACO-OFDM and DC-biased DMT schemes as a function of both the electrical and the optical energy per bit to single-sided noise power spectral density. However, the benefits are achieved at the expense of an increased transceiver complexity. As stated in [89], the approach is for further study under practical optical channel conditions.

8.6

System design and implementation aspects

8.6.1

Aspects of system design

So far, research and development on VLC using advanced LED modulation has focused on physical transmission basics, where usually a directed LOS is assumed. On the other hand, non-directed LOS links are more convenient in practical use, particularly if terminal mobility is desired. Non-directed indoor wireless IR channels have been extensively studied in the past by means of modeling, simulations, and experiments. Considering existing knowledge in this regard and similarities to VLC, such studies can provide adequate guidance for designing indoor VLC systems. However, there is only a little experience in practical terms of high-speed VLC via non-directed LOS and non-LOS links, i.e., links in diffuse scenarios.

Off-line experiments using a YB-LED and DC-biased DMT modulation in a realistic non-LOS broadcast configuration are presented e.g. in [90]. It is shown there that an area of

$\sim 18 \text{ m}^2$ can be covered with 100–200 Mbit/s, while the brightness level at the Rx equipped with a blue filter is about 500 lux (generated by an extra LED for lighting), and thus complies with workplace requirements. Some further results achieved for the first time with a real bidirectional system in a non-LOS configuration are presented below in Section 8.6.4.

Bidirectional links are a necessary condition for any kind of communication beyond broadcasting. Various approaches for an optical wireless indoor uplink have been discussed and the development of a quality uplink is currently one of the main research topics in this field. The most common approach, irrespective of the modulation format, is to use IR light as illustrated in Fig. 8.4. Examples of medium and high-speed systems are given e.g. in [20] and [91], respectively. However, visible light uplinks are also considered, as for instance shown in Fig. 8.5, given that a visible spot in the Rx region fits the application needs.

At the same time, bidirectional links enable dynamic adaptation to changing properties of the link, e.g. caused by ambient light or LOS blocking. The time-varying channel can easily be estimated using frequency domain channel estimation, and adaptive modulation can be applied based on the requested data rates and quality of service. The idea of OWC using DMT modulation with adaptive bit and power loading was proposed for the first time in [17] and independently thereof almost simultaneously in [18]. By this method, subcarriers are loaded with the best suitable modulation depending on the channel properties at individual frequencies, i.e., the power is distributed according to the SNR needs of each chosen modulation order or format while keeping the system constraints regarding BER and transmit power satisfied. This leads to optimal utilization of the available resources in a non-flat communication channel even in the presence of non-linear distortion caused by the transfer characteristics of common LEDs. The whole concept is analytically presented in [33, 34, 92]. Related algorithms for bit and power allocation are also addressed in [93], while experimental proofs of concept can be found in [94–96]. Further experimental studies have been performed according to [97] in order to demonstrate that the benefits of adaptively controlling the resultant QAM modulation orders also apply to YB-LED-based systems where blue filtering at the Rx is omitted.

In addition to channel adaptation, the possibility to combine DMT modulation with any *multiple access schemes* makes it an excellent preference for indoor VLC applications. Initial work directed toward multi-channel systems is published in [77] (see also [10]), where subcarrier multiplexing (SCM) is used to provide multi-user capability. The downlink capacity of an experimental setup based on off-line processing was assembled to 575 Mbit/s by wavelength division multiplexing (WDM) using the colored channels of a RGB-LED, while the YB-LED uplink of the full duplex system offered 225 Mbit/s. Pre- and post-equalization in the frequency domain were adopted to compensate for Tx and channel distortions. In addition, the transmission capacity was optimized using various QAM modulation orders. By adjusting the bandwidths and modulation formats of the sub-channels, the downlink and uplink capacities can be easily reconfigured in such a setup.

Regarding the *feeder or backhaul network* of VLC, a combination with the power line infrastructure and thus with PLC suggests itself, cf. for example [1, 2, 19, 98, 99]. From the viewpoint of DMT modulation used in both systems, this idea is of particular interest as it could simplify interfaces and interworking. Komine *et al.* proposed and analyzed an

integrated system of this kind in [100] based on their earlier work and subsequently, studies addressing that subject have been performed at several places. As an example, broadcasting the DMT-QAM signal of a PLC system by directly modulating the YB-LED of a VLC Tx was presented in [101]. More recent proposals for an integration of PLC and VLC can be found e.g. in [102]. For reasons of completeness, it has to be mentioned that optical fibers and DMT transmission can also serve for VLC backhauling. However, this creates a special area of research employing e.g. laser light, and thus will not be considered further here.

The interplay of VLC, backbone network and terminal systems also calls for an appropriate *media access control* (MAC) protocol. A specific MAC layer was proposed for the optical wireless channel (considering both visible light and IR applications) in the framework of the OMEGA project [103], see also Section 8.6.4. For VLC broadcast, a simplified frame format was described. At the Tx side of the considered system, the MAC layer provided a serial data stream at 100 Mbit/s for digital signal processing and modulation on the PHY layer. After transmission via VLC link and PHY processing at the Rx side, the retrieved data stream was passed to the MAC layer. An overview of the access method, the optical wireless data link layer (OWMAC) and the MAC frame adapted to that VLC prototype is given in [104]. All the modules for MAC and PHY processing at both the Tx and Rx side were implemented in FPGA technology [104, 105]. Apart from that work, multiple access schemes for multicarrier-based VLC channels are also addressed in e.g. [106, 107].

A major design challenge regarding the commercialization of VLC for joint use in lighting systems is how to incorporate the commonly used PWM *light dimming technique* while maintaining reliable high-speed communication links. In [108] this problem was considered in terms of VLC power constraints due to lighting requirements in living rooms for both daytime and night-time scenarios, i.e. even in the worst case of communication with the lights off. It was shown that very low light emission (virtually lights-off) is sufficient to maintain coverage at data rates up to the Mbit/s range using OOK or PPM. This leads to the conclusion that even if the average optical transmit power is severely dimmed and less power efficient modulation schemes such as DMT are used, there should be some electrical signal power for communication to a certain extent.

Regarding VLC systems based on DC-biased DMT or ACO-OFDM, dimming cannot be achieved directly, but the data signal finished for driving the LED can be combined with a dimming technique on the PHY layer. However, the simple way of multiplying the transmission signal and a PWM pulse train for dimming control during its “on” period is not an option, as the data throughput would be limited to the PWM rate, which is as low as a few 10 kHz in commercial LED lighting systems [12]. Achieving high-speed transmission with this approach is only feasible when the PWM dimming signal is at least twice the highest subcarrier frequency of the DMT signal to avoid subcarrier interference [21]. Such a constraint is hardly acceptable, as the LED modulation bandwidth should include the PWM frequency, which cuts the bandwidth for data transmission by 50%. Therefore, dimming schemes are being developed such as *reverse polarity* OFDM (RPO-OFDM), proposed in [109]. This method combines the high-frequency OFDM signal with the low-frequency PWM dimming signal, while both

Table 8.4 Key results of laboratory experiments using WDM in VLC systems based on DC-biased DMT.

Aggregate bit rate (Gbit/s)	Colors of WDM channels	Modulation bandwidth (MHz)	Number of subcarriers	Remarks	Reference
0.575	RG	50	64	PIN-Rx, 2 SCM channels per WDM channel, blue LED only used for lighting; in addition uplink via YB-LED	[10]
0.750	RGB	50	64	PIN-Rx, adaptive Nyquist windowing	[110]
0.803	RGB	50	32	APD-Rx	[111]
1.250	RGB	100	128	APD-Rx	[8]
2.930	RGB	230	471	PIN-Rx	[79]
3.400	RGB	280	512	APD-Rx	[9]

signals contribute to the effective LED brightness. RPO-OFDM utilizes the entire period of a PWM signal for data transmission by adjusting the polarity of the data symbols before they are superimposed on the PWM pulse train, which defines the dimming level, i.e. the symbol polarity is reversed during the “on” periods of the PWM signal. In this way, the data rate is maintained for a wide dimming range independently of the PWM frequency. The approach also keeps the signal within the dynamic range constraint of the LED. In conclusion, the data rate in RPO-OFDM is not limited by the PWM signal frequency, and the LED dynamic range is fully utilized to minimize the non-linear distortion of the multicarrier communication signal. This technique can be applied to any version of real-valued OFDM/DMT signal, preprocessed for transmission in VLC.

OFDM/DMT modulation continually gains in popularity due to its attractive communication performance, and the results achieved so far indicate that it is an excellent candidate for bidirectional transmission in VLC systems close to reality. Nevertheless, additional research is necessary, in particular to examine all aspects of cooperation with lighting systems and its effects on light quality in practical smart lighting scenarios.

8.6.2 DMT/OFDM application in advanced systems

When using RGB-type LEDs (or more generally, multi-color LED devices), a VLC system enables *wavelength division multiplexing* (WDM). To determine the potential of WDM in terms of transmission capacity, over recent years several laboratory studies on the WDM transmission performance in VLC systems have been carried out and reported. As a demonstration of bit rate per WDM channel was the main driver, spectrally efficient DC-biased DMT modulation was employed almost without exception.

Key results of laboratory experiments using WDM in VLC systems based on DC-biased DMT are given in Table 8.4, which indicates that bit rates of several 100 Mbit/s per WDM channel and total capacities in the Gbit/s range are possible.

It should be noted that all of these results have been achieved by exploring the WDM channels one by one and by means of off-line processing. In such a configuration, the

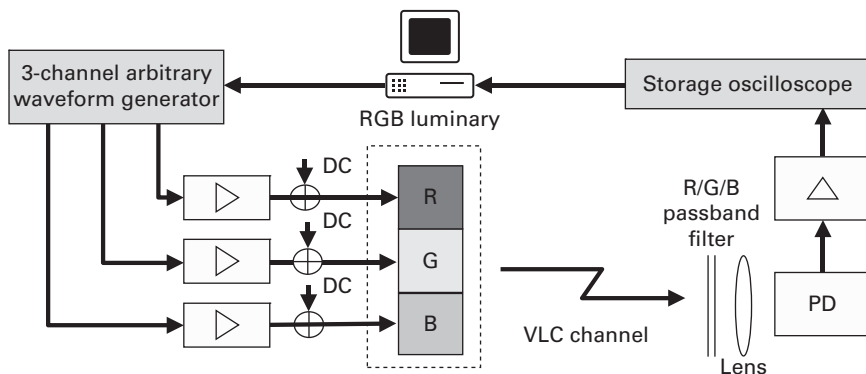


Figure 8.12 Setup for off-line evaluation of simultaneous DC-biased DMT transmission using three VLC channels in WDM fashion.

transmit signal is generated by software and an arbitrary waveform generator (AWG), while the received signal is recorded and subsequently evaluated by software. A typical setup of such an experiment is sketched in Fig. 8.12.

As VLC systems typically use multiple LEDs when combined with indoor lighting, it is an obvious step to apply the optical wireless *multiple-input multiple-output* (MIMO) principle in order to boost the overall transmission capacity. MIMO processing can compensate inter-channel crosstalk, thus allowing for parallel transmission from a number of LEDs [112]. In a corresponding optical MIMO proof of concept using AWG-generated DC-biased DMT modulation, a 2×2 Tx module consisting of four YB-LEDs, and a 3×3 -channel imaging Rx equipped with a blue filter, an aggregate bit rate of 1.1 Gbit/s has been demonstrated, as reported in [113].

Optical spatial modulation (OSM) is another bandwidth and power efficient MIMO scheme for OWC. It is based on multiple spatially separated Tx units and utilizes their location to carry extra information [114], i.e., in addition to applying basic signal modulation, OSM transmits further bits in the spatial domain by considering the Tx array as an extended constellation diagram. As only one Tx is active at any given time instant, the Rx unit can easily determine the index of an active Tx and thus can be kept simple. In the case of aligned Tx and Rx units, it was shown that the paths of the optical MIMO channel are nearly uncorrelated. Thus, an accurate Tx-Rx alignment results in a power efficiency increase with respect to the modulation scheme used. A comprehensive overview of the state of the art in spatial modulation for MIMO technologies, including application in VLC, is provided e.g. by [115]. A novel unipolar modulation method for OWC based on OSM is introduced in [116]. It combines the basic spatial modulation scheme and OFDM techniques for OWC [69]. Results show that the new approach improves the power efficiency. For the same spectral efficiency, it exhibits 5 to 9 dB higher energy efficiency than ACO-OFDM, while in contrast to DC-biased DMT it eliminates the need for a DC bias. Consequently, it exhibits a considerable power efficiency gain for the same spectral efficiency.

8.6.3 Practical implementation issues

With the aim of reducing the *DSP complexity* at both the Tx and the Rx, IFFT/FFT processing can be replaced by a discrete Hartley transform (DHT) [117, 85]. DHT is a real-valued self-inverse transform without Hermitian symmetry constraint at the input. As a result, there is no need for complex algebra and the same fast DSP algorithm can be used for modulation and demodulation as well, if real constellations are used for subcarrier modulation. Real-time implementations of DHT-based Tx and Rx thus have confirmed a reduction of both complexity and computing time, while the performance is the same as in DFT-based DC-biased DMT and ACO-OFDM systems, respectively [117].

An important goal of VLC in general is to drive the LED at the best possible electro-optical power conversion efficiency. Additionally in dual use with lighting, the illumination function must be maintained with minimum extra power consumption. In most cases, VLC designs try to employ (digital) off-the-shelf *high-power LED drivers* [109], and also to use the dimming capability usually offered by such devices. An outline of the important role of LED drivers in smart lighting systems can be found in [2], while the LED driver's energy efficiency along with the OOK, VPPM and OFDM modulation schemes is discussed in [118]. Usually, the large current of high-power LEDs controlled by the driver circuit severely degrades its response. In [38] it is shown that OOK-based systems nonetheless can achieve rather sound energy efficiency while enabling transmission rates of 477 Mbit/s. In this case, the red device of a RGB-LED was driven by a specially designed circuit with pre-emphasis, which improved the 3 dB bandwidth of the optical Tx to 91 MHz. Another approach to a simple and practical LED driver providing a high overall Tx-bandwidth is based on drawing out the remaining carriers that exist in the LED depletion capacitance during the “off” state of the OOK input signal [119].

These examples for OOK modulation indicate that it appears unrealistic to use standard driver circuits in OFDM/DMT-based systems, which exploit the bandwidth more efficiently but need more complex analog circuitry, usually along with higher power consumption. Because the optical Tx performance depends, *inter alia*, strongly on the driver output impedance, careful impedance matching to the LED device or module is of utmost importance. As a typical example, Fig. 8.13 illustrates the bandwidth of an optical Tx including high-power LED and customized analog circuitry, which can drive currents up to 1.2 A. Such a driver was employed in various VLC setups using either a RGB-LED [8] or a YB-LED including blue filter [77, 120]. Compared to pure lighting, an increased power consumption of about 30% is observed when changing to VLC operation at the same brightness level at the Rx. In view of such power values, RF leakage can be stronger than the received optical signal. That is why accurate RF shielding of the VLC Tx in any case is an important subject.

Beyond the modulation scheme used in a VLC system, convenient ways for performance improvement are equalization at the Tx (pre-equalization), at the Rx (post-equalization), or a combination of such techniques. As an example, pre-equalization can be a part of the LED driving module [29].

Post-equalization is briefly addressed below. A noise cancellation method for an ACO-OFDM Rx is presented in [121], where the anti-symmetry of the time domain signal

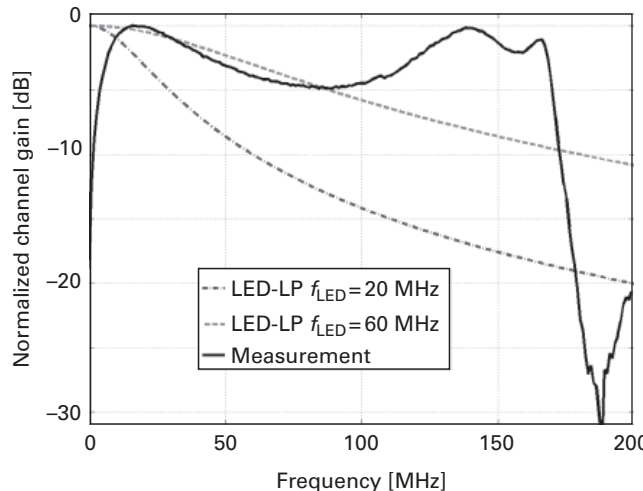


Figure 8.13 VLC channel response taken with a network analyzer at a short distance from a high-power YB-LED, which was driven by a custom-tailored analog driver circuit at a bias current of 0.7 A. The effective modulation bandwidth was about 180 MHz. For comparison simulated first order RC low-pass LED amplitude responses are also shown [120].

samples inherent in ACO-OFDM is used to identify which samples of the received signal are most likely to be due to the addition of noise. These samples are then set to zero. A maximum gain of 3 dB in optical power can be achieved with this method. The same pairwise maximum likelihood (ML) Rx structure can be employed in PAM-DMT systems by considering their anti-symmetry properties. It is worth mentioning that the use of this Rx technique in a system based on flip-OFDM results in the U-OFDM scheme as presented in [84], cf. Sections 8.5.3 and 8.5.4. In another case, post-processing is proposed to eliminate the effect of noise outside the maximum channel delay by means of a least square (LS) channel estimation method [122]. The scheme is based on a comb-type pilot subcarrier arrangement, where each OFDM symbol has pilot tones at periodically-located subcarriers. After ordinary LS channel estimation, the derived channel is truncated in the time domain according to the maximum channel delay via DFT and inverse DFT, respectively. In this way, the method can significantly improve the BER performance, as has been proved by simulation at different QAM constellation orders in a DC-biased DMT system.

Apart from the limited modulation bandwidth, white LEDs suffer from intrinsic non-linearity. This effect is particularly detrimental when high PAPR modulation formats such as DMT are employed. Much work has been done to overcome this impairment, cf. Section 8.3.3. In [123], the application of Volterra equalization is proposed for compensating ISI and the YB-LED non-linearity in a VLC system that employs M -PAM modulation. It was demonstrated that a Rx using a decision feedback equalizer (DFE) with non-linear Volterra feed-forward section up to the second order can efficiently compensate effects of non-linearity of the transmitting LED and performs up to 5 dB

better in terms of optical power than using a standard DFE. In view of such results, this scheme is also attractive for DMT-based VLC systems.

It is hardly surprising that the SNR distribution in an area covered by indoor VLC can be improved, as well as the spectral efficiency of the DMT-based modulation, by tilting the (moving) receiver plane. Such a scheme has been proposed in [124] to enhance the performance in an adaptive system, where a feedback channel is used to adapt bit and power loading. The optimum tilting angle of the photodetector is determined by the Newton method, which is a fast algorithm requiring a three-step search from the initial state.

Up to now, experimental comparisons of different system approaches and details thereof are extremely scarce. Quite recently, the bit rate performances of various VLC approaches, including DC-biased DMT, ACO-OFDM, and U-OFDM have been experimentally compared in [125]. Clearly, the bandwidth efficiency of DC-biased DMT presents a higher bit rate performance, but is of course less power efficient than ACO-OFDM. On the other hand, the ACO-OFDM as well as the U-OFDM schemes suffer from the effect of baseline wander in practical transmission, caused by the moving average of the asymmetric signal. Such findings require closer examination in future work.

8.6.4

Implementation and demonstration

The feasibility of white LED intensity modulation using OFDM was validated for the first time by experimental results as published in [126]. Since then, a lot of research and analytical work, as well as simulations and experimental studies on DMT/OFDM-based VLC, including subsystems thereof as discussed above, have been carried out. Despite this, there are only a very small number of system implementations which incorporate real-time signal processing for DMT/OFDM modulation, etc. This is however mandatory for system verification under real-life conditions and an important step for paving the way to real commercial application.

An early proof-of-concept hardware demonstrator is shown in Fig. 8.14, where the bandwidth of 45 kHz was limited by the DSP development kit used for performing OFDM-related signal processing. The aim of this system was to study the performance of phase-incoherent optical OFDM under various conditions, e.g. against different electrical SNRs. Moreover, the system served for characterization of the wireless channel and for modeling.

In the course of the European research and development project OMEGA, a fully-fledged high-speed VLC system based on DMT modulation has been developed and implemented, which offers wireless broadcast channels of 100 Mbit/s (net) in homes [129]. Under real-life conditions such a performance was demonstrated for the first time in February 2011, by broadcasting up to four HD video streams (80% utilization of the 100 Mbit/s channel) simultaneously from a total of 16 YB-LED ceiling lamps to a photodetector placed anywhere within the lit area of about 10 m². An illustration is given in Fig. 8.15. The MAC protocol (Optical Wireless MAC) developed especially for this purpose, and digital signal processing functionalities for the PHY layer, were implemented on FPGA boards. The PHY processing encompassed a typical DMT modulator/demodulator including scrambler and forward error correction (FEC)

Table 8.5 Digital PHY parameters of the fully-fledged VLC demonstrator.

Parameter	Value
Signal bandwidth (MHz)	30.5947
Number of subcarriers (incl. DC)	32
Length of cyclic prefix (samples)	4
QAM order	16
FEC (Reed Solomon)	187 207

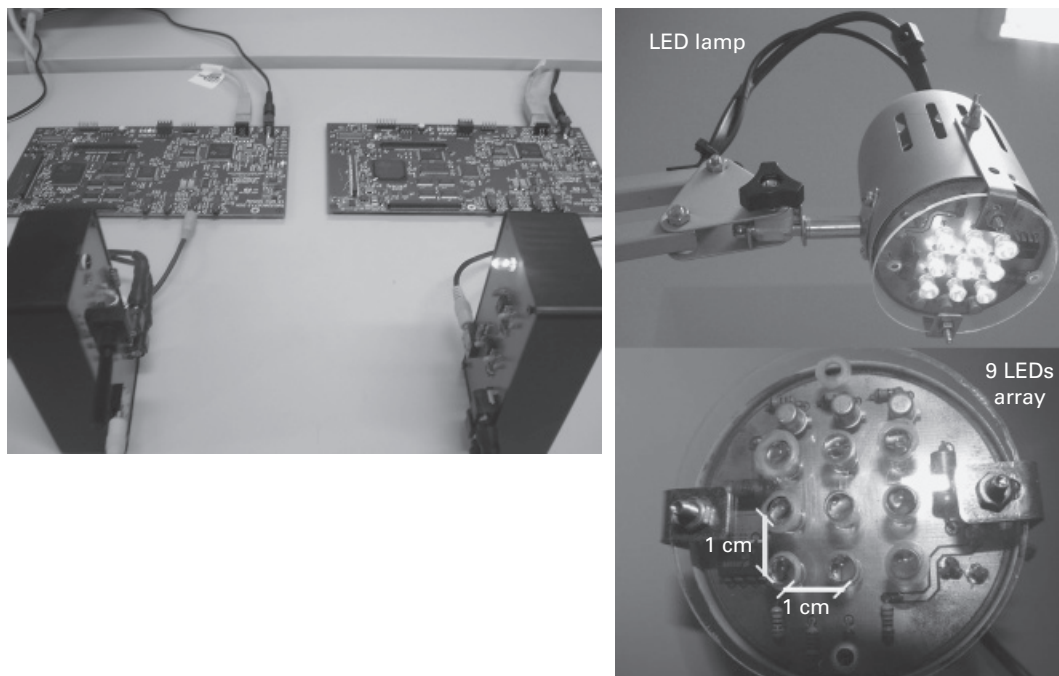


Figure 8.14 *Left:* Laboratory VLC demonstrator for initial unidirectional OFDM-based real-time experiments [127]. *Right:* Reading lamp with an array of nine white LEDs in order to enlarge the coverage area for OFDM experiments [128].

encoder/decoder with parameters summarized in Table 8.5. The physical layer also featured full synchronization on bit and frame levels [104, 130, 131].

More recently at Fraunhofer HHI, a bidirectional high-speed real-time VLC system has been presented (Fig. 8.16), which operates in a time division duplex mode. Rate-adaptive DC-biased DMT is implemented by feedback via the reverse link. The transceivers are equipped with proprietary VLC Tx and Rx modules providing a modulation bandwidth of up to 180 MHz. However, the bandwidth used is below 100 MHz, limited by the DSP chips. These transceiver modules can operate without active cooling and offer 1000BASE-T Ethernet interfaces, cf. Fig. 8.16 (bottom).



Figure 8.15 The first public demonstration of a high-speed VLC system using DMT modulation for broadcasting multiple video streams at a data rate of 100 Mbit/s (125 Mbit/s gross data rate at PHY layer). (*Top*) Array of VLC transmitters on the ceiling; (*bottom*) mobile receiver device consisting of a photodetector and an amplifier for forwarding the signal to the demodulator and further to the video screens.

A particular advantage of this real-time VLC system is the variable throughput of up to 500 Mbit/s with controlled BER, depending on the quality of the optical communication channel. The system offered the first mobile VLC experience. As shown in Fig. 8.17, the most important parameter is the light intensity at the Rx, leading to an almost proportional data rate adaptation. It should be noted that the observed



Figure 8.16 (Top): Two bidirectional transceivers communicating via a diffuse link. Different colors are used for down and uplink as an example, but also the same colors can be used. (Bottom left): View of the diffusing spot of the link at a (standard painted) wall at a distance of up to ~3 m from the transceivers. The overall link length is about 6 m. (Bottom right): New generation of bidirectional transceiver with a form factor of $87 \times 114 \times 42$ mm³ (without lenses).

performance is similar with illumination LEDs of any color. IR-LEDs can be used as well as white light phosphorous LEDs, which benefit from built-in pre-equalization and thus do not require blue filtering at the Rx. The power consumption of this system is only moderately increased – by 30% compared to the original lighting function – due to an optimized LED driver design.

Figure 8.17 reveals another important result: *high-speed non-LOS data transmission*. In this particular case, light was reflected by the white-painted wall to the Rx. More than 100 Mbit/s are possible at a link range of about 3 m, despite diffusion through reflection.

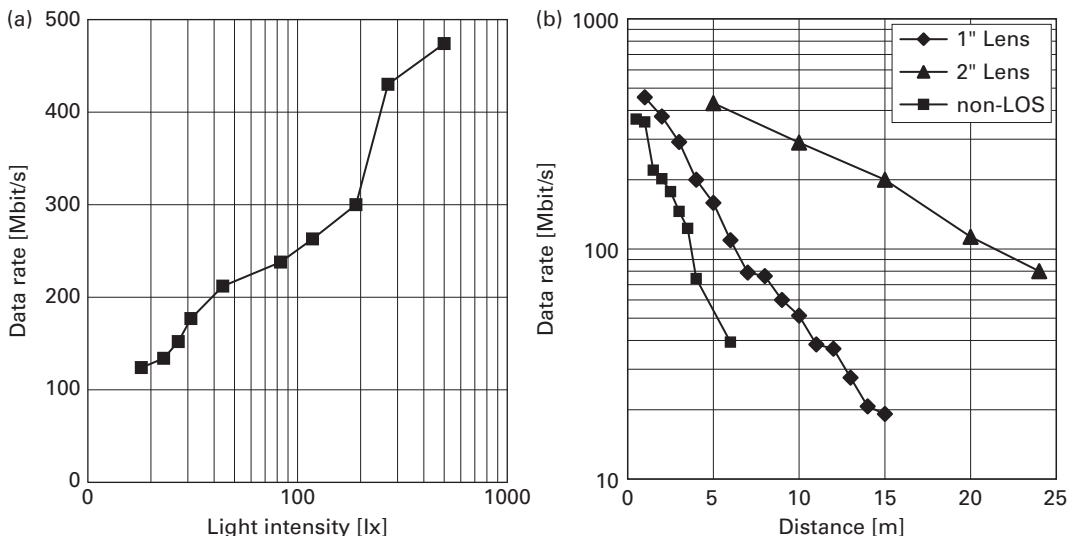


Figure 8.17 (a) Maximum achieved data rates with the real-time rate-adaptive VLC system depending on the light intensity at the Rx. (b) Maximum data rates achieved with different link types: LOS link with narrow FOV (triangle curve), LOS link with wide FOV (diamond curve), and a non-LOS diffuse link (square curve).

In this way, the feasibility of a flexible and robust VLC connection was demonstrated at high bit rates under different link scenarios.

A similar implementation was published recently in [91]. This VLC system used a YB-LED device for the downlink and an IR uplink, with an integrated OFDM-based DSP chip for real-time operation. The LED bandwidth of ~ 1 MHz has been increased to ~ 12 MHz by an analog pre-equalization technique without using a blue filter. The modulation bandwidth of the DSP chip applied is between 2 and 30 MHz and the adaptive OFDM modulation uses formats from QPSK to 16-QAM. This system offers a data throughput up to 37 Mbit/s over about 1.5 m distance.

From all demonstrations discussed above it can be concluded that rate-adaptive systems based on DMT modulation, as also used in radio and wired transmission, can be implemented with off-the-shelf components. It has been shown that such systems are an excellent solution for robust optical wireless-link systems with peak data rates up to 500 Mbit/s under various lighting conditions. Nonetheless, the commercially available DSP chips, which of course are not intended for application in VLC systems, or solutions extensively tailored on FPGA, respectively, limit the data rate and the overall system performance. Moreover, there are limits in optimization of important parameters such as power consumption. Full custom integrated circuits using current technology would be able to remove such shortcomings but would require entering the mass market.

These experiments and measurements using real-time adaptive bidirectional VLC systems fulfill an important intermediate step to turn the optical WiFi vision into reality.

The next steps will integrate VLC technology into real-life room lighting, and will implement extensions such as Mp-to-Mp functionality.

8.7

Summary

In this chapter, the use of DMT modulation schemes in VLC for indoor application is presented along with the most important features and conditions. Items of VLC are discussed with focus on the provision of high-speed links using DMT-based modulation, i.e. only as far as there are special requirements of system design in that respect. In accordance with the present status of research and development on OWC around the world, the PHY layer is emphasized in this chapter.

Against this backdrop, the optical wireless channel is briefly characterized, and methods to exploit its capacity by means of typical high-brightness LEDs intended for lighting in combination with DMT-based modulation and IM/DD transmission are presented. Properties of the basic DMT/OFDM versions, namely DC-biased DMT, ACO-OFDM and PAM-DMT are discussed and compared. Moreover, several variants of these schemes for use in VLC systems are highlighted. In a nutshell, DMT/OFDM modulation is identified as a method of choice for exploiting VLC channels of restricted bandwidth due to the LED device and the driver characteristics. The modulation schemes are able to take advantage of the high SNR that is available in VLC scenarios based on room lighting and typical brightness levels. A further important advantage is the ability to adapt the modulation format of each subcarrier to the SNR of the channel, commonly known as bit and power loading. Such an advanced exploitation of the channel capacity also provides flexibility in coverage, but it requires a feedback link.

In addition, it has been shown that DMT modulation can also be applied to most advanced VLC transmission schemes using WDM and MIMO techniques. By means of WDM the transmission capacity can be multiplied, however, multi-color LEDs as well as more complex or colored Rx units are necessary in such a scenario. Higher bit rates are also possible using MIMO technologies. Related research is in an early phase but at a high level of activity.

The numerous comparative analyses of the DMT/OFDM modulation formats show that both of the basic schemes using asymmetrical clipping, i.e., ACO-OFDM and PAM-DMT, are best at low spectral efficiency and high power efficiency, i.e. where power consumption rather than bit rate is of importance. Their computational complexity is nearly the same. However, these schemes as well as variants proposed and under discussion have not yet left the laboratory stage due to the difficulty of real-time implementation, which is mandatory for VLC verification under conditions such as mobility. On the other hand, DC-biased DMT has the lowest computational complexity among the three major DMT/OFDM modulation formats. The scheme is expected to offer the highest data rate in applications, where the additional DC bias power required in VLC to create a non-negative modulation signal can provide a complementary functionality, such as illumination. In fact, the record-breaking results in transmission rate as presented in [8, 9, 11, 46] have all been achieved using DC-biased DMT. The first implementations and transceiver

prototypes, as far as they have been made public, also use DC-biased DMT including real-time signal processing, thus enabling a mobile VLC experience. According to this, the suitability of DMT modulation for robust indoor VLC application at high data rates has been confirmed already by real-life verification and public demonstration.

It is also important to note that the poor modulation bandwidth of white light LEDs of the YB-type is not an issue any more. It has been demonstrated that the blue filter, which mitigates the adverse effect of the phosphor layer but is unfavorable concerning the power budget, can be replaced by equalization. In that way, the optical power reaching the Rx can be fully exploited at bit rates of several 100 Mbit/s or even more.

Although DMT-based modulation has continually gained in popularity due to its attractive performance, various versions of single-carrier frequency domain equalization (SCFDE) transmission move into the VLC spotlight. These techniques offer reduced PAPR, which may result in an overall better performance [132, 133]. Newly, DC-biased DMT and SCFDE transmission have been compared in a WDM experimental setup, where aggregate data rates of 2.5 Gbit/s and 3.75 Gbit/s respectively, have been achieved [134]. Hence, the SCFDE scheme clearly outperformed DMT in that setup. Another single-carrier modulation scheme, namely carrier-less amplitude and phase (CAP) modulation has been explored too [79]. An aggregate bit rate of 3.22 Gbit/s, again achieved in a WDM experiment, confirms the significance of single-carrier modulation as an important option for high-speed VLC systems. Ways for further performance improvement on PHY level may also be opened by a quasi balanced detection scheme for OFDM signals, recently introduced in [135].

So far work on both VLC and LED-based lighting has focused on vital issues of each individual domain. More specifically, lifetime, color, luminous efficacy, etc. of devices have been subjects investigated in LED lighting development, while topics such as LED modulation and driving, related signal processing and link control have been addressed in communications. True VLC system design, however, needs multi-disciplinary work covering communications and lighting technology as well. For example, LED long-term behavior under VLC operation including a potentially high PAPR needs to be verified, as so far there is only initial experience. Regarding LED modulation and power supplies, it may be useful to drive LED lamps as an integral part of the existing infrastructure directly with AC-power. Basic results on such a VLC approach, yet at low speed and using OOK, have been published recently in [136]. Additional research is also necessary to examine LED modulation effects on light quality in practical smart lighting scenarios. As is correctly pointed out in [12] for the dual-use case, VLC and light intensity control are in conflict. Thus, it is important to consider DMT-compatible (hybrid) dimming schemes in extended VLC standards. They should also take into account emerging standards on radio and wired transmission, which are closely related from the VLC systems point of view. It is an open issue whether lighting and energy demands will be met in all respects. Thus, this presents a field for further studies. More verification in real environments is also necessary, which calls for joint work by the communications and lighting industries.

Several VLC techniques have been verified by experiments with reliable off-line processing and also by a few demonstrations using components off the shelf. Real

low-cost systems now need custom designed devices, such as integrated DSP for optimization of VLC performance and features to be considered, as stated in this chapter. In this matter, interaction with DSP chip manufacturers is necessary along with ongoing work of standardization at the system level.

Finally, it must be mentioned that system integration has been considered only at a rudimentary level so far and mobility-related issues such as handover in VLC have not been adequately addressed. Moreover, a dedicated standardization roadmap is essential for future availability of VLC in portable devices [137]. Standardization activities so far emanate from the Infrared Data Association (IrDA) interest group and from the IEEE. Whereas the IrDA mainly provides specifications for wireless infrared protocols, the IEEE has published a first OWC standard, IEEE 802.15.7–2011, for VLC. The recent extension of the International Telecommunication Union (ITU) g.hn standard (ITU-T Recommendation G.9960, 2011) foreseeing an optical channel is also of importance, cf. [102], concerning integration of VLC, e.g. into home networks and cooperation with present infrastructure.

Even if there are still challenges as named above, which are being faced by research and development, VLC presents a realistic and promising supplementary technology to radio communication.

References

- [1] M. Kavehrad, “Sustainable energy-efficient wireless applications using light,” *IEEE Communications Magazine*, **48**, (12), 66–73, 2010.
- [2] A. Sevincer, A. Bhattacharai, M. Bilgi, M. Yuksel, and N. Pala, “LIGHTNETS: Smart lighting and mobile optical wireless networks – a survey,” *IEEE Communications Surveys & Tutorials*, **15**, (4), 1620–1641, 2013.
- [3] S. Haruyama, “Visible light communication using sustainable LED lights,” Proceedings of 5th ITU Kaleidoscope: *Building Sustainable Communities*, 2013.
- [4] L. Hanzo, H. Haas, S. Imre, *et al.*, “Wireless myths, realities, and futures: From 3G/4G to optical and quantum wireless,” *Proceedings of the IEEE*, **100**, 1853–1888, 2012.
- [5] D.K. Borah, A.C. Boucouvalas, C.C. Davis, S. Hramilovic, and K. Yiannopoulos, “A review of communication-oriented optical wireless systems,” *EURASIP Journal on Wireless Communications and Networking*, **91**, 1–28, 2012.
- [6] K.-D. Langer, J. Hilt, D. Schulz, *et al.*, “Rate-adaptive visible light communication at 500 Mb/s arrives at plug and play,” *Optoelectronics and Communications* SPIE Newsroom, DOI 10.1117/2.1201311.005196, 2013.
- [7] J. Vučić, C. Kottke, S. Nerrreter, *et al.*, “230 Mbit/s via a wireless visible-light link based on OOK modulation of phosphorescent white LEDs,” *OFC/NFOEC Technical Digest* 2010, paper OThH3.
- [8] C. Kottke, J. Hilt, K. Habel, J. Vučić, and K.-D. Langer, “1.25 Gbit/s visible light WDM link based on DMT modulation of a single RGB LED luminary,” Proc. European Conference and Exhibition on *Optical Communication (ECOC)* 2012, paper We.3.B.4.

- [9] G. Cossu, A.M. Khalid, P. Choudhury, R. Corsini, and E. Ciaramella, “3.4 Gbit/s visible optical wireless transmission based on RGB LED,” *Optics Express*, **20**, (26), B501–B506, 2012.
- [10] Y. Wang, Y. Shao, H. Shang, *et al.*, “875-Mb/s asynchronous bi-directional 64QAM-OFDM SCM-WDM transmission over RGB-LED-based visible light communication system,” *OFC/NFOEC Technical Digest* 2013, paper OTh1G.3.
- [11] D. Tsonev, H. Chun, S. Rajbhandari, *et al.*, “A 3-Gb/s single-LED OFDM-based wireless VLC link using a Gallium Nitride μ LED,” *IEEE Photonics Technology Letters*, **26**, (7), 637–640, 2014.
- [12] J. Gancarz, H. Elgala, and T.D.C. Little, “Impact of lighting requirements on VLC systems,” *IEEE Communications Magazine*, **51**, (12), 34–41, 2013.
- [13] R.D. Roberts, S. Rajagopal, and S.-K. Lim, “IEEE 802.15.7 physical layer summary,” Proc. IEEE GLOBECOM Workshops 2011, pp. 772–776.
- [14] S. Rajagopal, R.D. Roberts, and S.-K. Lim, “IEEE 802.15.7 visible light communication: Modulation schemes and dimming support,” *IEEE Comm. Mag.*, **50**, (3), 72–82, 2012.
- [15] D. Tsonev, S. Videv, and H. Haas, “Light fidelity (Li-Fi): Towards all-optical networking,” Proc. SPIE **9007**, *Broadband Access Communication Technologies VIII*, 900702, 2013.
- [16] J.M. Kahn and J.R. Barry, “Wireless infrared communications,” *Proceedings of the IEEE*, **85**, (2), 265–298, 1997.
- [17] J. Grubor, V. Jungnickel, K.-D. Langer, and C. v. Helmolt, “Dynamic data-rate adaptive signal processing method in a wireless infra-red data transfer system,” Patent EP1897252 B1, 24 June 2005.
- [18] O. Gonzalez, R. Perez-Jimenez, S. Rodriguez, J. Rabadan, and A. Ayala, “OFDM over indoor wireless optical channel,” *IEE Proc. Optoelectronics*, **152**, (4), 199–204, 2005.
- [19] L. Grobe, A. Paraskevopoulos, J. Hilt, *et al.*, “High-speed visible light communication systems,” *IEEE Communications Magazine*, **51**, (12), 60–66, 2013.
- [20] Z. Ghassemlooy, H. Le Minh, P.A. Haigh, and A. Burton, “Development of visible light communications: Emerging technology and integration aspects,” Proc. *Optics and Photonics Taiwan International Conference (OPTIC)*, 2012.
- [21] G. Ntogari, T. Kamalakis, J.W. Walewski, and T. Sphicopoulos, “Combining illumination dimming based on pulse-width modulation with visible-light communications based on discrete multitone,” *Journal of Optical Comm. and Networking*, **3**, (1), 56–65, 2011.
- [22] J. Grubor, S.C.J. Lee, K.-D. Langer, T. Koonen, and J. Walewski, “Wireless high-speed data transmission with phosphorescent white-light LEDs,” Proc. European Conference and Exhibition on *Optical Communication (ECOC)* 2007, **6**, Post-Deadline Paper PD3.6.
- [23] C.W. Chow, C.H. Yeh, Y.F. Liu, and Y. Liu, “Improved modulation speed of LED visible light communication system integrated to main electricity network,” *El. Letters*, **47**, (15), 2011.
- [24] Y. Pei, S. Zhu, H. Yang, *et al.*, “LED modulation characteristics in a visible-light communication system,” *Optics and Photonics Journal*, **3** (2B), 139–142, 2013.
- [25] J. Grubor, S. Randel, K.-D. Langer, and J.W. Walewski, “Broadband information broadcasting using LED-based interior lighting,” *J. of Lightwave Tech.*, **26**, (24), 3883–3892, 2008.
- [26] J. Armstrong, R.J. Green, and M.D. Higgins, “Comparison of three receiver designs for optical wireless communications using white LEDs,” *IEEE Communications Letters*, **16**, (5), 748–751, 2012.
- [27] D.C. O’Brien, L. Zeng, H. Le-Minh, *et al.*, “Visible light communications,” in R. Kraemer, M.D. Katz (eds.), *Short-Range Wireless Communications*, pp. 329–342, Wiley & Sons Ltd., 2009.
- [28] C.W. Chow, C.H. Yeh, Y. Liu, and Y.F. Liu, “Digital signal processing for light emitting diode based visible light communication,” *IEEE Phot. Society Newsletter*, **26**, (5), 9–13, 2012.

- [29] H. Le-Minh, D.C. O'Brien, G. Faulkner, *et al.*, "80 Mbit/s visible light communications using pre-equalized white LED," Proc. 34th European Conference and Exhibition on *Optical Communication (ECOC)*, 2008.
- [30] J. Vučić, C. Kottke, S. Nerreter, K.-D. Langer, and J.W. Walewski, "513 Mbit/s visible light communications link based on DMT-modulation of a white LED," *Journal of Lightwave Technology*, **28**, (24), 3512–3518, 2010.
- [31] H. Chun, C.-J. Chiang, and D.C. O'Brien, "Visible light communication using OLEDs: Illumination and channel modeling," Int. Workshop on *Optical Wireless Communications (IWOW)*, 2012.
- [32] P.A. Haigh, Z. Ghassemlooy, I. Papakonstantinou, and H. Le Minh, "2.7 Mb/s with a 93 kHz white organic light emitting diode and real time ANN equalizer," *IEEE Photonics Technology Letters*, **25**, (17), 1687–1690, 2013.
- [33] J. Grubor and K.-D. Langer, "Efficient signal processing in OFDM-based indoor optical wireless links," *Journal of Networks*, **5**, (2), 197–211, 2010.
- [34] J. Vučić, "Adaptive modulation technique for broadband communication in indoor optical wireless systems," PhD Thesis at Technische Universitaet Berlin, Germany, 2009.
- [35] X. Li, J. Vučić, V. Jungnickel, and J. Armstrong, "On the capacity of intensity-modulated direct-detection systems and the information rate of ACO-OFDM for indoor optical wireless applications," *IEEE Transactions on Communications*, **60**, (3), 799–809, 2012.
- [36] S. Dimitrov and H. Haas, "Information rate of OFDM-based optical wireless communication systems with nonlinear distortion," *J. of Lightwave Tech.*, **31**, (6), 918–929, 2013.
- [37] X. Zhang, K. Cui, M. Yao, H. Zhang, and Z. Xu, "Experimental characterization of indoor visible light communication channels," Proc. 8th International Symposium on *Communication Systems, Networks & Digital Signal Processing (CSNDSP)*, 2012.
- [38] N. Fujimoto and H. Mochizuki, "477 Mbit/s visible light transmission based on OOK-NRZ modulation using a single commercially available visible LED and a practical LED driver with a pre-emphasis circuit," *OFC/NFOEC Technical Digest* 2013, paper JTh2A.73.
- [39] I. Neokosmidis, T. Kamalakis, J.W. Walewski, B. Inan, and T. Sphicopoulos, "Impact of nonlinear LED transfer function on discrete multitone modulation: Analytical approach," *Journal of Optical Communications and Networking*, **1**, (5), 439–451, 2009.
- [40] I. Stefan, H. Elgala, R. Mesleh, D. O'Brien, and H. Haas, "Optical wireless OFDM system on FPGA: Study of LED nonlinearity effects," Proc. 73rd IEEE *Vehicular Technology Conference (VTC Spring)*, pp. 1–5, 2011.
- [41] S.-B. Ryu, J.-H. Choi, J. Bok, H. Lee, and H.-G. Ryu, "High power efficiency and low nonlinear distortion for wireless visible light communication," Proc. 4th IFIP International Conference on *New Technologies, Mobility and Security (NTMS)*, pp. 1–5, 2011.
- [42] D. Lee, K. Choi, K.-D. Kim, and Y. Park, "Visible light wireless communications based on predistorted OFDM," *Optics Communications*, **285**, (7), 1767–1770, 2012.
- [43] D. Tsonev, S. Sinanovic, and H. Haas, "Complete modeling of nonlinear distortion in OFDM-based optical wireless communication," *Journal of Lightwave Technology*, **31**, (18), 3064–3076, 2013.
- [44] R. Mesleh, H. Elgala, and H. Haas, "LED nonlinearity mitigation techniques in optical wireless OFDM communication systems," *Journal of Optical Communications and Networking*, **4**, (11), 865–875 , 2012.
- [45] R. Mesleh, H. Elgala, and H. Haas, "On the performance of different OFDM based optical wireless communication systems," *Journal of Optical Communications and Networking*, **3**, (8), 620–628, 2011.

- [46] A.M. Khalid, G. Cossu, R. Corsini, P. Choudhury, and E. Ciaramella, “1-Gb/s transmission over a phosphorescent white LED by using rate-adaptive discrete multitone modulation,” *IEEE Photonics Journal*, **4**, (5), 1465–1473, 2012.
- [47] B. Inan, S.C.J. Lee, S. Randel, *et al.*, “Impact of LED nonlinearity on discrete multitone modulation,” *Journal of Optical Communications and Networking*, **1**, (5), 439–451, 2009.
- [48] C. Ma, H. Zhang, K. Cuib, M. Yaoa, and Z. Xu, “Effects of LED lighting degradation and junction temperature variation on the performance of visible light communication,” International Conference on Systems and Informatics (ICSAI), pp. 1596–1600, 2012.
- [49] J.B. Carruthers and J.M. Kahn, “Multiple-subcarrier modulation for non-directed wireless infrared communication,” *IEEE J. on Selected Areas in Comm.*, **14**, (3), 538–546, 1996.
- [50] Y. Tanaka, T. Komine, S. Haruyama, and M. Nakagawa, “A basic study of optical OFDM system for indoor visible communication utilizing plural white LEDs as lighting,” 8th Int. Symp. on Microwave and Optical Technol. (ISMOT), pp. 303–306, 2001.
- [51] J. Armstrong and A.J. Lowery, “Power efficient optical OFDM,” *Electronics Letters*, **42**, (6), 370–372, 2006.
- [52] S.C.J. Lee, S. Randel, F. Breyer, and A.M.J. Koonen, “PAM-DMT for intensity-modulated and direct-detection optical communication systems,” *IEEE Photonics Technology Letters*, **21**, (23), 1749–1751, 2009.
- [53] S. Randel, F. Breyer, and S.C.J. Lee, “High-speed transmission over multimode optical fibers,” Proc. 34th European Conference and Exhibition on *Optical Communication (ECOC)* 2008, paper OWR2.
- [54] J.M. Cioffi, “A multicarrier primer,” *ANSI Contribution TIE1*, **4**, 91–157, 1991.
- [55] J. Armstrong, “OFDM for optical communications,” *Journal of Lightwave Technology*, **27**, (3), 189–204, 2009.
- [56] A.V. Oppenheim and R.W. Schafer, *Discrete-Time Signal Processing*, Prentice-Hall, 1989.
- [57] S.K. Hashemi, Z. Ghassemlooy, L. Chao, and D. Benhaddou, “Orthogonal frequency division multiplexing for indoor optical wireless communications using visible light LEDs,” Proc. 6th Int. Symp. on *Communication Systems, Networks & Digital Signal Processing (CSNDSP)* 2008, pp. 174–178.
- [58] J. Armstrong, B.J.C. Schmidt, D. Kalra, H.A. Suraweera, and A.J. Lowery, “Performance of asymmetrically clipped optical OFDM in AWGN for an intensity modulated direct detection system,” Proc. IEEE Global Telecommunications Conf. (GLOBECOM ’06), SPC07–4, 2006.
- [59] S.C.J. Lee, F. Breyer, S. Randel, H.P.A. van den Boom, and A.M.J. Koonen, “High-speed transmission over multimode fiber using discrete multitone modulation,” *Journal of Optical Networking*, **7**, (2), 183–196, 2008.
- [60] E. Vanin, “Signal restoration in intensity-modulated optical OFDM access systems,” *Optics Letters*, **36**, (22), 4338–4340, 2011.
- [61] X. Li, R. Mardling, and J. Armstrong, “Channel capacity of IM/DD optical communication systems and of ACO-OFDM,” Proc. Int. Conf. on *Communications (ICC)* 2007, pp. 2128–2133, 2007.
- [62] S.K. Wilson and J. Armstrong, “Transmitter and receiver methods for improving asymmetrically-clipped optical OFDM,” *IEEE Trans. on Wireless Comm.*, **8**, (9), 4561–4567, 2009.
- [63] S.C.J. Lee, F. Breyer, S. Randel, *et al.*, “Discrete multitone modulation for maximizing transmission rate in step-index plastic optical fibers,” *Journal of Lightwave Technology*, **27**, (11), 1503–1513, 2009.

- [64] L. Chen, B. Krongold, and J. Evans, "Performance analysis for optical OFDM transmission in short-range IM/DD systems," *Journal of Lightwave Technology*, **30**, (7), 974–983, 2012.
- [65] S. Tian, K. Panta, H.A. Suraweera, *et al.*, "A novel timing synchronization method for ACO-OFDM-based optical wireless communications," *IEEE Transactions on Wireless Communications*, **7**, (12), 4958–4967, 2008.
- [66] M.M. Freda and J.M. Murray, "Low-complexity blind timing synchronization for ACO-OFDM-based optical wireless communications," Proc. IEEE GLOBECOM Workshops 2010, pp. 1031–1036.
- [67] R. You and J.M. Kahn, "Average power reduction techniques for multiple subcarrier intensity-modulated optical signals," *IEEE Trans. Communications*, **49**, (12), 2164–2171, 2001.
- [68] B. Ranjha and M. Kavehrad, "Precoding techniques for PAPR reduction in asymmetrically clipped OFDM based optical wireless system," Proc. SPIE **8645**, *Broadband Access Communication Technologies VII*, **86450R**, 2013.
- [69] J. Armstrong and B.J.C. Schmidt, "Comparison of asymmetrically clipped optical OFDM and DC-biased optical OFDM in AWGN," *IEEE Comm. Letters*, **12**, (5), 343–345, 2008.
- [70] D.J.F. Barros, S.K. Wilson, and J.M. Kahn, "Comparison of orthogonal frequency-division multiplexing and pulse-amplitude modulation in indoor optical wireless links," *IEEE Transactions on Communications*, **60**, (1), 153–163, 2012.
- [71] S. Dimitrov, S. Sinanovic, and H. Haas, "Signal shaping and modulation for optical wireless communication," *Journal of Lightwave Technology*, **30**, (9), 1319–1328, 2012.
- [72] S.D. Dissanayake and J. Armstrong, "Comparison of ACO-OFDM, DCO-OFDM and ADO-OFDM in IM/DD systems," *Journal of Lightwave Technology*, **31**, (7), 1063–1072, 2013.
- [73] Z. Yu, R.J. Baxley, and G.T. Zhou, "EVM and achievable data rate analysis of clipped OFDM signals in visible light communication," *EURASIP Journal on Wireless Communications and Networking*, (1), 1–16, 2012.
- [74] L. Chen, B. Krongold, and J. Evans, "Theoretical characterization of nonlinear clipping effects in IM/DD optical OFDM systems," *IEEE Transactions on Communications*, **60**, (8), 2304–2312, 2012.
- [75] S. Dimitrov, S. Sinanovic, and H. Haas, "Clipping noise in OFDM-based optical wireless communication systems," *IEEE Trans. on Communications*, **60**, (4), 1072–1081, 2012.
- [76] C.W. Chow, C.H. Yeh, Y.F. Liu, and P.Y. Huang, "Background optical noises circumvention in LED optical wireless systems using OFDM," *IEEE Phot. J.*, **5**, (2), 7900709, 2013.
- [77] C. Kottke, K. Habel, L. Grobe, *et al.*, "Single-channel wireless transmission at 806 Mbit/s using a white-light LED and a PIN-based receiver," Proc. 14th Int. Conf. on *Transparent Optical Networks* (ICTON), paper We.B4.1, 2012.
- [78] Y. Wang, Y. Wang, N. Chi, J. Yu, and H. Shang, "Demonstration of 575-Mb/s downlink and 225-Mb/s uplink bi-directional SCM-WDM visible light communication using RGB LED and phosphor-based LED," *Optics Express*, **21**, (1), 1203–1208, 2013.
- [79] F.M. Wu, C.T. Lin, C.C. Wei, *et al.*, "Performance comparison of OFDM signal and CAP signal over high capacity RGB-LED-based WDM visible light communication," *IEEE Photonics Journal*, **5**, (4), 7901507, 2013.
- [80] S.D. Dissanayake, K. Panta, and J. Armstrong, "A novel technique to simultaneously transmit ACO-OFDM and DCO-OFDM in IM/DD systems," Proc. IEEE GLOBECOM Workshops 2011, pp. 782–786.
- [81] K. Asadzadeh, A.A. Farid, and S. Hranilovic, "Spectrally factorized optical OFDM," Proc. 12th Canadian Workshop on *Information Theory* (CWIT), pp. 102–105, 2011.

- [82] N. Fernando, Y. Hong, and E. Viterbo, "Flip-OFDM for optical wireless communications," *Proc. Information Theory Workshop (ITW)*, 5–9, 2011.
- [83] Y.-I. Jun, "Modulation and demodulation apparatuses and methods for wired / wireless communication," Patent WO/2007/064165, 2007.
- [84] D. Tsonev, S. Sinanovic, and H. Haas, "Novel unipolar orthogonal frequency division multiplexing (U-OFDM) for optical wireless," IEEE 75th *Vehicular Technology Conference (VTC Spring)*, pp. 1–5, 2012.
- [85] A. Nuwanpriya, A. Grant, S.-W. Ho, and L. Luo, "Position modulating OFDM for optical wireless communications," *Proc. 3rd IEEE Workshop on Optical Wireless Communications (OWC'12)*, pp. 1219–1223, 2012.
- [86] L. Chen, B. Krongold, and J. Evans, "Diversity combining for asymmetrically clipped optical OFDM in IM/DD channels," *Proc. IEEE Global Telecomm. Conf. (GLOBECOM '09)*, pp. 1–6, 2009.
- [87] S.D. Dissanayake, J. Armstrong, and S. Hranilovic, "Performance analysis of noise cancellation in a diversity combined ACO-OFDM system," *Proc. 14th Int. Conf. on Transparent Optical Networks (ICTON)*, 2012.
- [88] M.Z. Farooqui and P. Saengudomlert, "Transmit power reduction through subcarrier selection for MC-CDMA-based indoor optical wireless communications with IM/DD," *EURASIP Journal on Wireless Communications and Networking*, (1), 1–14, 2013.
- [89] R. Zhang and L. Hanzo, "Multi-layer modulation for intensity modulated direct detection optical OFDM," *J. of Optical Communications and Networking*, 5, (12), 1402–1412, 2013.
- [90] G. Cossu, A.M. Khalid, R. Corsini, and E. Ciaramella, "Non-directed line-of-sight visible light system," *OFC/NFOEC Technical Digest* 2013, paper OTh1G.2.
- [91] C.H. Yeh, Y.-L. Liu, and C.-W. Chow, "Real-time white-light phosphor-LED visible light communication (VLC) with compact size," *Opt. Express*, 21, (22), 26192–26197, 2013.
- [92] J. Grubor, V. Jungnickel, and K.-D. Langer, "Adaptive optical wireless OFDM system with controlled asymmetric clipping," *IEEE Proc. 41st Asilomar Conference on Signals, Systems and Computers*, 2007.
- [93] Z. Sun, Y. Zhu, and Y. Zhang, "The DMT-based bit-power allocation algorithms in the visible light communication," *Proc. 2nd International Conference on Business Computing and Global Informatization*, pp. 572–575, 2012.
- [94] K.-D. Langer, J. Vučić, C. Kottke, *et al.*, "Advances and prospects in high-speed information broadcast," *Proc. 11th Int. Conf. on Transparent Optical Networks (ICTON)*, paper Mo.B5.3, 2009.
- [95] J. Vučić, C. Kottke, S. Nerreter, *et al.*, "White light wireless transmission at 200+ Mb/s net data rate by use of discrete-multitone modulation," *IEEE Photonics Technology Letters*, 21, (20), 1511–1513, 2009.
- [96] D. Bykhovsky and S. Arnon, "An experimental comparison of different bit-and-power-allocation algorithms for DCO-OFDM," *Journal of Lightwave Technology*, 32, (8), 1559–1564, 2014.
- [97] C.W. Chow, C.H. Yeh, Y.F. Liu, P.Y. Huang, and Y. Liu, "Adaptive scheme for maintaining the performance of the in-home white-LED visible light wireless communications using OFDM," *Optics Communications*, 292, (1), 49–52, 2013.
- [98] K.L. Sterckx, "Implementation of continuous VLC modulation schemes on commercial LED spotlights," *Proc. 9th International Conference on Electrical Engineering/Electronics, Computer, Telecommunications and Information Technology (ECTI-CON)*, 2012.

- [99] H. Elgala, R. Mesleh, and H. Haas, "Indoor optical wireless communication: Potential and state-of-the-art," *IEEE Communications Magazine*, **49**, (9), 56–62, 2011.
- [100] T. Komine, S. Haruyama, and M. Nakagawa, "Performance evaluation of narrowband OFDM on integrated system of power line communication and visible light wireless communication," Proc. 1st Int. Symp. on *Wireless Pervasive Computing*, 2006.
- [101] S.E. Alavi, A.S.M. Supa'at, S.M. Idrus, and S.K. Yusof, "New integrated system of visible free space optic with PLC," Proc. 3rd Workshop on *Power Line Communications (WSPLC)*, 2009.
- [102] H. Ma, L. Lampe, and S. Hranilovic, "Integration of indoor visible light and power line communication systems," Proc. 17th IEEE International Symposium on *Power Line Communications and its Applications (ISPLC)*, pp. 291–296, 2013.
- [103] K.-D. Langer, J. Grubor, O. Bouchet, *et al.*, "Optical wireless communications for broadband access in home area networks," Proc. 10th Int. Conf. on *Transparent Optical Networks (ICTON)*, **4**, 149–154, 2008.
- [104] O. Bouchet, P. Porcon, and E. Gueutier, "Broadcast of four HD videos with LED ceiling lighting: Optical-wireless MAC," Proc. SPIE **8162**, *Free-Space and Atmospheric Laser Communications XI*, 81620L, 2011.
- [105] O. Bouchet, P. Porcon, J.W. Walewski, *et al.*, "Wireless optical network for a home network," Proc. SPIE **7814**, *Free-Space Laser Communications X*, 781406, 2010.
- [106] M.V. Bhalerao, S.S. Sonavane, and V. Kumar, "A survey of wireless communication using visible light," *Int. Journal of Advances in Engineering & Technology*, **5**, (2), 188–197, 2013.
- [107] J. Dang and Z. Zhang, "Comparison of optical OFDM-IDMA and optical OFDMA for uplink visible light communications," Proc. International Conference on *Wireless Communications & Signal Processing (WCSP)*, 2012.
- [108] T. Borogovac, M.B. Rahaim, M. Tuganbayeva, and T.D.C. Little, "Lights-off visible light communications," Proc. IEEE GLOBECOM Workshops 2011, pp. 797–801.
- [109] H. Elgala and T.D.C. Little, "Reverse polarity optical-OFDM (RPO-OFDM): Dimming compatible OFDM for gigabit VLC links," *Optics Express*, **21**, (20), 24288–24299, 2013.
- [110] R. Li, Y. Wang, C. Tang, *et al.*, "Improving performance of 750-Mb/s visible light communication system using adaptive Nyquist windowing," *Chinese Optics Letters*, **11**, (8), 080605/1–4, 2013.
- [111] J. Vučić, C. Kottke, K. Habel, and K.-D. Langer, "803 Mbit/s visible light WDM link based on DMT modulation of a single RGB LED luminary," *OFC/NFOEC Technical Digest* 2011, paper OWB6.
- [112] A.H. Azhar, T.-A. Tran, and D. O'Brien, "Demonstration of high-speed data transmission using MIMO-OFDM visible light communications," Proc. IEEE GLOBECOM Workshops 2010, pp. 1052–1056.
- [113] A.H. Azhar, T.-A. Tran, and D. O'Brien, "A gigabit/s indoor wireless transmission using MIMO-OFDM visible-light communications," *IEEE Photonics Tech. Letters*, **25**, 171–174, 2013.
- [114] X. Zhang, S. Dimitrov, S. Sinanovic, and H. Haas, "Optimal power allocation in spatial modulation OFDM for visible light communications," Proc. IEEE 75th *Vehicular Technology Conference (VTC Spring)*, pp. 1–5, 2012.
- [115] X. Di Renzo, H. Haas, A. Ghayeb, S. Sugiura, and L. Hanzo, "Spatial modulation for generalized MIMO: Challenges, opportunities, and implementation," *Proceedings of the IEEE*, **102**, (1), 56–103, 2014.

- [116] Y. Li, D. Tsonev, and H. Haas, “Non-DC-biased OFDM with optical spatial modulation,” Proc. IEEE 24th Int. Symp. on Personal, Indoor and Mobile Radio Communications (PIMRC), pp. 486–490, 2013.
- [117] M.S. Moreolo, R. Muñoz, and G. Junyent, “Novel power efficient optical OFDM based on Hartley transform for intensity-modulated direct-detection systems,” *Journal of Lightwave Technology*, **28**, (5), 798–805, 2010.
- [118] G. del Campo Jiménez and F.J. López Hernández, “VLC oriented energy efficient driver techniques,” Proc. SPIE **8550**, *Optical Systems Design* 2012, 85502F.
- [119] T. Kishi, H. Tanaka, Y. Umeda, and O. Takyu, “A high-speed LED driver that sweeps out the remaining carriers for visible light communications,” *Journal of Lightwave Technology*, **32**, (2), 239–249, 2014.
- [120] L. Grobe and K.-D. Langer, “Block-based PAM with frequency domain equalization in visible light communications,” Proc. IEEE GLOBECOM Workshops 2013, pp. 1075–1080, 2013.
- [121] K. Asadzadeh, A. Dabbo, and S. Hranilovic, “Receiver design for asymmetrically clipped optical OFDM,” Proc. IEEE GLOBECOM Workshops 2011, pp. 777–781.
- [122] X. Yang, Z. Min, T. Xiongyan, W. Jian, and H. Dahai, “A post-processing channel estimation method for DCO-OFDM visible light communication,” Proc. 8th Int. Symp. on Communication Systems, Networks & Digital Signal Processing (CSNDSP), 2012.
- [123] G. Stepniak, J. Siuzdak, and P. Zwierko, “Compensation of a VLC phosphorescent white LED nonlinearity by means of Volterra DFE,” *IEEE Photonics Technology Letters*, **25**, (16), 1597–1600, 2013.
- [124] Z. Wang, C. Yu, W.-D. Zhong, and J. Chen, “Performance improvement by tilting receiver plane in M-QAM OFDM visible light communications,” *Optics Express*, **19**, (14), 13418–13427, 2011.
- [125] A.H. Azhar and D. O’Brien, “Experimental comparisons of optical OFDM approaches in visible light communications,” Proc. IEEE GLOBECOM Workshops 2013, pp. 1076–1080, 2013.
- [126] M.Z. Afgani, H. Haas, H. Elgala, and D. Knipp, “Visible light communication using OFDM,” Proc. 2nd International Conference on Testbeds and Research Infrastructures for the Development of Networks and Communities (TRIDENTCOM), pp. 129–134, 2006.
- [127] H. Elgala, R. Mesleh, H. Haas, and B. Pricope, “OFDM visible light wireless communication based on white LEDs,” Proc. 65th IEEE Vehicular Technol. Conf. (VTC Spring), pp. 2185–2189, 2007.
- [128] H. Elgala, R. Mesleh, and H. Haas, “Indoor broadcasting via white LEDs and OFDM,” *IEEE Transactions on Consumer Electronics*, **55**, (3), 1127–1134, 2009.
- [129] J. Vučić, L. Fernández, C. Kottke, K. Habel, and K.-D. Langer, “Implementation of a real-time DMT-based 100 Mbit/s visible-light link,” Proc. European Conference and Exhibition on Optical Communication (ECOC) 2010, paper We.7.B.1.
- [130] K.-D. Langer, J. Vučić, C. Kottke, et al., “Exploring the potentials of optical-wireless communication using white LEDs,” Proc. 13th Int. Conf. on Transparent Optical Networks (ICTON), paper Tu.D5.2, 2011.
- [131] J. Vučić and K.-D. Langer, “High-speed visible light communications: State-of-the-art,” *OFC/NFOEC Technical Digest* 2012, paper OTh3G.3.
- [132] M. Wolf, L. Grobe, M.R. Rieche, A. Koher, and J. Vučić, “Block transmission with linear frequency domain equalization for dispersive optical channels with direct detection,” Proc. 12th Int. Conf. on Transparent Optical Networks (ICTON), paper Th.A3.4, 2010.

- [133] K. Acolatse, Y. Bar-Ness, and S.K. Wilson, “Novel techniques of single-carrier frequency-domain equalization for optical wireless communications,” *EURASIP Journal on Advances in Signal Processing*, 2011, article ID 393768.
- [134] N. Chi, Y. Wang, Y. Wang, X. Huang, and X. Lu, “Ultra-high-speed single red-green-blue light-emitting diode-based visible light communication system utilizing advanced modulation formats,” *Chinese Optics Letters*, **12**, (1), 010605/1–4, 2014.
- [135] Y. Wang, N. Chi, Y. Wang, *et al.*, “High-speed quasi-balanced detection OFDM in visible light communication,” *Optics Express*, **21**, (23), 27558–27564, 2013.
- [136] Y.F. Liu, C.H. Yeh, C. W. Chow, and Y.L. Liu, “AC-based phosphor LED visible light communication by utilizing novel signal modulation,” *Optical and Quantum Electronics*, **45**, (10), 1057–1061, 2013.
- [137] G. Dede, T. Kamalakis, and D. Varoutas, “Evaluation of optical wireless technologies in home networking: an analytical hierarchy process approach,” *Journal of Optical Communications and Networking*, **3**, (11), 850–859, 2011.